FUZZY SLIDING MODE CONTROL FOR CART INVERTED PENDULUM SYSTEM

BELAL AHMED ABDELAZIZ ELSAYED

FACULTY OF ENGINEERING
UNIVERSITY OF MALAYA
KUALA LUMPUR

2013

FUZZY SLIDING MODE CONTROL FOR CART INVERTED PENDULUM SYSTEM

BELAL AHMED ABDELAZIZ ELSAYED

THESIS SUBMITTED IN FULFILLMENT OF THE REQUIREMENTS FOR THE DEGREE OF MASTER OF ENGINEERING SCIENCE

FACULTY OF ENGINEERING
UNIVERSITY OF MALAYA
KUALA LUMPUR

2013

Abstract

Cart Inverted Pendulum (CIP) is a benchmark problem in nonlinear automatic control which has numerous applications, such as two wheeled mobile robot and under actuated robots. The objective of this study is to design a swinging-up controller with a robust sliding mode stabilization controller for CIP, and to apply the proposed controller on a real CIP. Two third-order differential equations were derived to create a combining model for the cart-pendulum with its DC motor dynamics, where the motor voltage is considered as the system input. The friction force between the cart and rail was included in the system equations through a nonlinear friction model. A Fuzzy Swinging-up controller was designed to swing the pendulum toward the upright position, with consideration of the cart rail limits. Once the pendulum reaches the upward position, Sliding Mode Controller (SMC) is activated, to balance the system. For comparison purposes, a Linear Quadratic Regulator Controller (LQRC) was design and compared with proposed SMC. Simulation and experimental results have shown a significant improvement of the proposed SMC over LQRC where, the pendulum angle oscillations were decreased by 80% in the real implementation.

Abstrak

Troli bandul Inverted (CIP) sistem adalah masalah penanda aras dalam kawalan automatik linear. Terdapat banyak aplikasi untuk CIP dalam kehidupan kita, seperti dua robot beroda mudah alih yang dianggap sebagai pengangkutan era peribadi baru. Tujuan kajian ini ialah untuk merekabentuk pengawal berayun-up dengan pengawal penstabilan mantap untuk CIPS dan memohon pengawal kepada sistem sebenar. Dalam mod sistem, dua persamaan pembezaan tertib ketiga diperoleh untuk mewujudkan satu model yang menggabungkan untuk bandul cart dengan motor dinamik DC. Dalam model yang dibentangkan voltan motor dianggap sebagai input sistem dan semua batasan praktikal dianggap. Daya geseran antara cart dan rel telah dimasukkan ke dalam sistem persamaan melalui model geseran tak linear. A Fuzzy berayun-up pengawal telah direka untuk ayunan bandul untuk kedudukan tegak dalam pertimbangan had rel cart. Setelah bandul mencapai kedudukan menaik, Ketiga-perintah gelongsor Mod Pengawal (SMC) diaktifkan, untuk mengimbangi sistem. Dalam usaha untuk mengesahkan prestasi SMC dicadangkan Pengawal Pengawal Selia Linear kuadratik (LQRC) telah dicadangkan dan berbanding dengan cadangan SMC. Simulasi dan eksperimen keputusan telah menunjukkan peningkatan yang ketara SMC dicadangkan lebih LQRC mana, sudut ayunan bandul telah menurun sebanyak 80% dalam pelaksanaan sebenar.

Acknowledgment

"Allah taught you that which you knew not. And Ever Great is the Grace of Allah unto you" (Surat Al-Nisa verse 113)

First, I want to thank ALLAH for his Grace and for giving me the strength to finish this work. Thanks for my supervisors Prof. Saad Mekhelif and Ass.Prof. Mohsen Abdelnaiem for their patience, guidance and encouragement during all my studying stages. I am also grateful for their confidence and freedom they gave during this work.

Special thanks go to my big family, my parent and my siblings, for their kind help and understanding. Also I want to express my gratitude to Aalaa, my wife, for her continues support during two years of a hard work.

Finally, I would like to thank all my colleagues in the University of Malaya for this great time of exchanging knowledge and experiences.

Table of Contents

List of Figures

List of Tables

List of Abbreviation

IP: Inverted Pendulum

CIP: Cart-Inverted Pendulum

SMC: Sliding Mode Controller

CW: Clock Wise

CCW: Counter Clock Wise

FLC: Fuzzy Logic Control

KBFC: Knowledge Based Fuzzy Control

FBL: Feedback Linearization.

PID: Proportional–integral–derivative

CG: Center of Gravity

LQRC: Linear Quadratic Regulator Controller

DC: Direct Current

EMF: Elector Magnetic Force

PC: Personal Computer

AD/DA: Analog to Digital/Digital to Analog

SISO: Single-Input Single-Output

SIMO: Single-Input Multi-Output

List of Symbols

X Cart displacement

θ Pendulum angle

$\dot{X}$ Cart velocity

$\dot{\theta}$ Pendulum Angular velocity

$\ddot{X}$ Cart acceleration

$\ddot{\theta}$ Pendulum angular acceleration

V_a DC motor applied voltage

i DC motor armature current

L_a DC motor armature Inductance

R_a DC motor armature resistance

ω DC Motor angular velocity

T_e DC Motor torque

T_j DC Motor inertia torque

T_B DC Motor damping torque

T_L DC Motor load torque

M Cart Mass

m Pendulum mass

L Pendulum length (From the pivot to the center of gravity)

F Applied force on the cart

F_{fr} Friction force between the cart and the rail

q Friction coefficient between the pendulum and the pivot

I Pendulum mass moment of inertia around the C.G

J DC motor rotor mass moment of inertia

K_t Motor Torque constant

K_e Back EMF constant

r DC Motor pulley Diameter

B Motor rotor damping coefficient

F_S Static Friction force

F_C Coulumb Friction force

X_{d} Dead zone velocities

V_S Stribeck velocity

n Friction form factor

b Viscous friction coefficient.

Chapter one

1 Introduction

1.1 Introduction

Controlling of nonlinear systems could be classified into two main categories. In the first one, the system is approximated into linear model, where the classical control theories are applied directly. This method of analysis is much simpler since it avoids dealing with the complicated mathematics due to systems nonlinearity. The global stability cannot be achieved because of neglecting the nonlinear effects.

On the other hand, nonlinear control techniques are applied to guarantee the global stability and to improve the system response. Advanced mathematical tools are necessitated to analyze the exact nonlinear models, and for stability guarantee (Khalil, 2002).

1.2 Inverted Pendulum System

Inverted Pendulum (IP) is an essential bench mark problem in nonlinear control. It is a challenging problem for control engineers because of system nonlinearity and instability. IP is a normal pendulum in the upright position which could be controlled by moving the pivot point in the horizontal plan. Swinging up and stabilization of IP is a fundamental problem in control field. In this task, the pendulum is swung from the downward (stable) position to

the upward (unstable) position. Then, the stabilization controller is applied to keep the pendulum stable in that position, as it is shown in Figure 1.1 (Rubi et al., 2002).

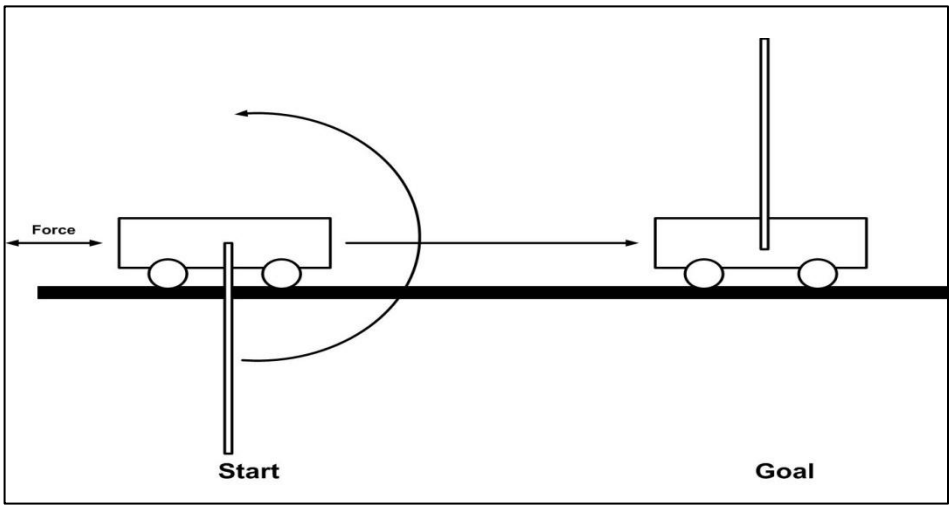

Figure 1.1: Inverted pendulum swinging-up

In the real life, there are many applications for IP, for example, two wheeled mobile robot which is known commercially as Segway robot, Figure 1.2. This robot model is similar to IP where, the pendulum and the pivot are replaced with the robot body and the two-wheels, respectively. The wheels are power-driven by an electric motor to keep the robot stable (Cardozo andVera, 2012) .

Figure 1.2: Segway robot(Segway, 2012)

Nowadays, Segway has been utilized in airports, malls, ect, by the security guards and workers, in order to save their time and efforts. It is expected to be the new era personal transports during the next decades (Voth, 2005) . Rockets and missiles are considered as IP applications, where the system is unstable during the initial stage of flight. Controlling of IP might be used to be applied in rockets to control the throttle angle.

Further application for IP is under-actuated robot, which is defined as "the robot which have number of actuators fewer than its degrees of freedoms"(Wang et al., 2007). The main advantage of reducing the actuators number is to minimize the power consumptions; also it leads to more compatible design where the weight and size are significantly reduced. Figure 1.3 and Figure 1.4 show two examples of underactuated robots, rat and flying robots. IP system is considered as an under actuated system because only one actuator is used to control both of the pendulum and the pivot point. Therefore, IP is used as platform for under- actuated robots control (Tedrake, 2009).

Figure 1.3: Flying under actuated robots (Tedrake, 2009).

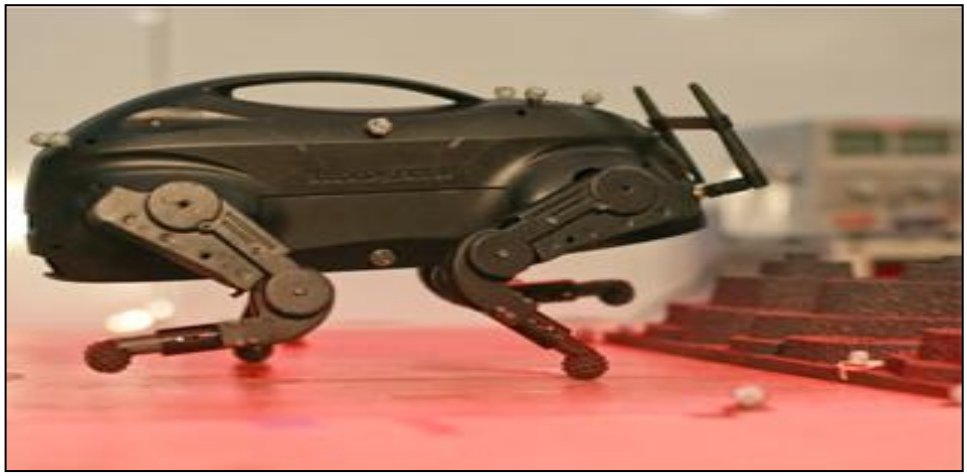

Figure 1.4: Rat under actuated robot (Tedrake, 2009).

In control laboratories, two types of IP could be found, based on the pivot point motion, linear or angular. In linear type, the pivot point is fixed to a cart which moves on horizontally on a rail, the cart is driven by an electrical motor (usually DC motor). This type is well known as Cart-Inverted Pendulum (CIP), Figure 1.5 (Das andPaul, 2011) . In the angular type, the pivot motion is angular and it is also driven by an electric motor. It is sometimes known as Futura Pendulum (Japanese scientist), see Figure 1.6 (Shiriaev et al., 2007). Swinging-up of CIP is more challengeable because of the cart rail limits, in contrast to Furuta pendulum where the pivot motion is boundless.

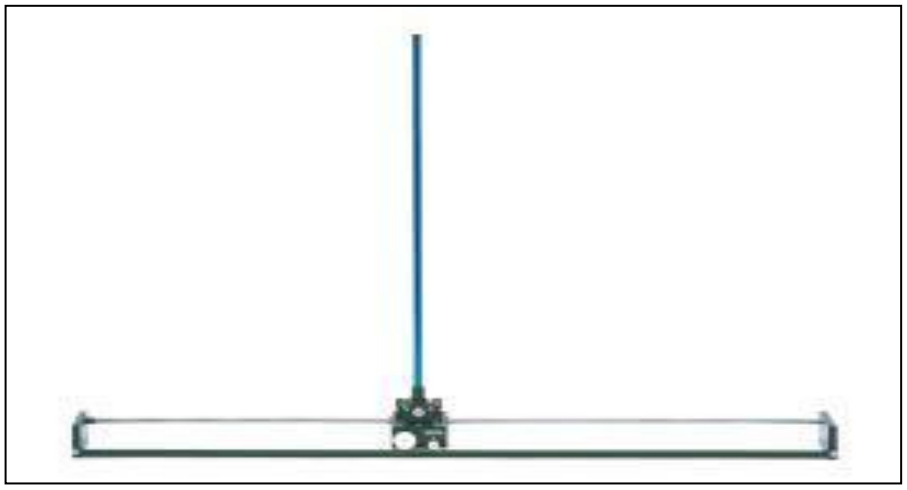

Figure 1.5: Cart Inverted Pendulum

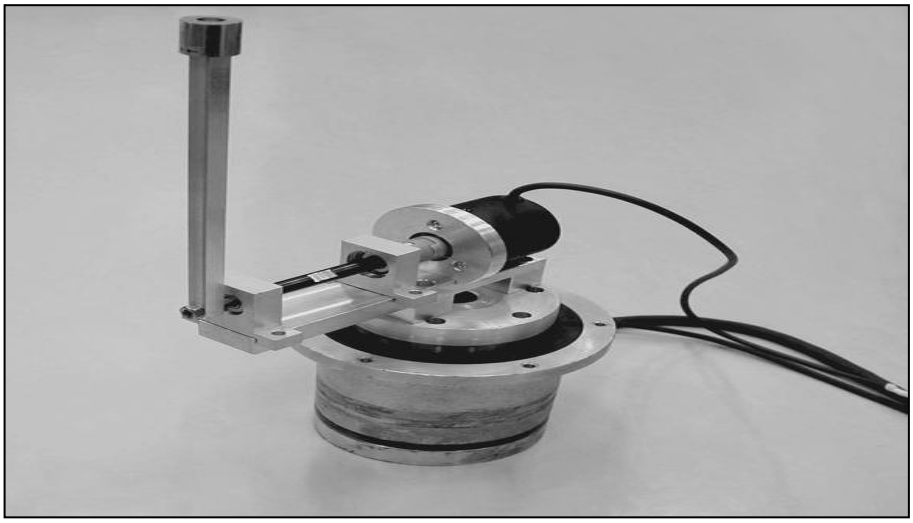

Figure 1.6: Furuta Pendulum (Buckingham, 2003).

1.3 Fuzzy Logic Control

Fuzzy Logic Control (FLC) has been introduced as an alternative tool for nonlinear complex systems. It is also known as Knowledge Based Fuzzy Control (KBFC) because of using the human knowledge. The fuzzy control algorithm consists of linguistic expressions in form of IF-THEN rules. The rules are designed based on the human experience and knowledge.

Fuzzy logic and fuzzy sets were introduced by Lotfy Zadeh in 1960s (L. A. Zadeh, 1965; Lotfi A. Zadeh, 1973). Fuzzy control process is divided into three main sequences: fuzzification, decision making and defuzzification, see Figure 1.7. Fuzzification process converts the real or crisp inputs value into the fuzzy value, based on the membership functions. The controller decision is taken based on the human experience through IF-THEN rules. Finally, in deffuzification stage, the controller output is converted back to the physical value.

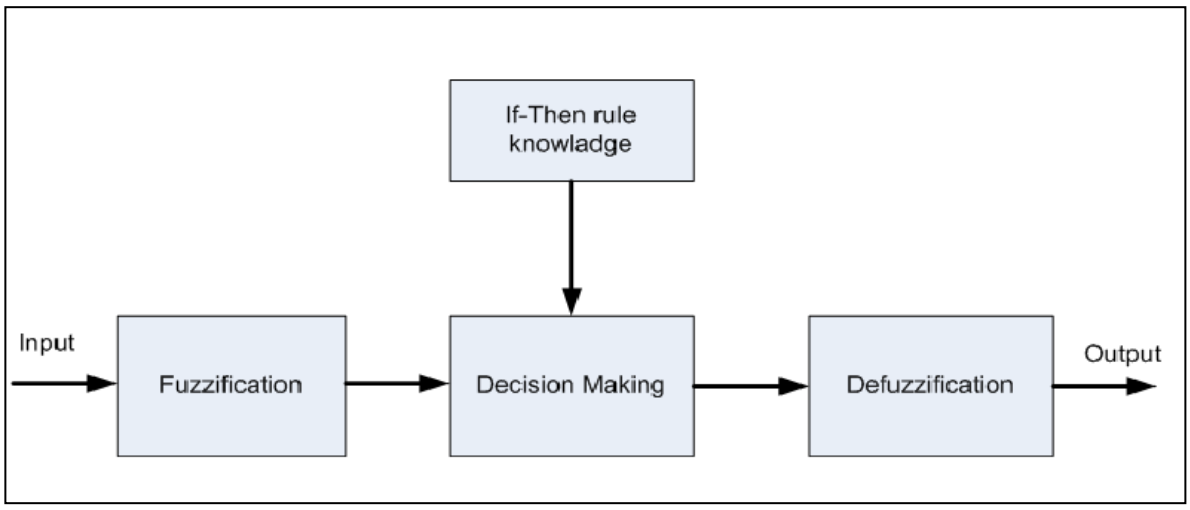

Figure 1.7: Fuzzy control process.

FLC control has been applied widely for many engineering applications. However, it has some drawbacks in analyzing some complicated systems where the numbers of rules are increased. (Passino andYurkovich, 1998). In this study, a fuzzy controller will be applied to swing the pendulum up under the cart rail restrictions.

1.4 Sliding Mode Control

Sliding mode control technique provides a robust control tool that deals with nonlinear systems. It was initially developed in Soviet Union during the early of 1960s (Edwards andSpurgeon, 1998; Itkis, 1976; Utkin, 1977). Recently, sliding mode has been extensively applied in many engineering aspects e.g., Robotics, aerodynamics and power electronic (Liang andJianying, 2010; Siew-Chong et al., 2008; Xiuli et al., 2010).

The main advantages of sliding mode are: 1) Stability guarantees 2) robustness under system parameters variation. 3) External disturbances rejection. 4) Fast dynamic response. However, sliding mode has a drawback of chattering problem (high frequencies in the control signal) which might cause actuators failure. Numbers of solutions have been introduced to decrease the chattering effects (Boiko andFridman, 2005; Mondal et al., 2012; Young andDrakunov, 1992).

The Sliding Mode Controller (SMC) design consists of two parts: the sliding surface and the control law. The control law is designed to force the system states to move towards the sliding surface. Once the sliding surface is reached, the system state will slide on the surface till it reaches the stability point (Yorgancioglu andKomurcugil, 2010). In this project, SMC is used to design a stabilization controller CIP to keep the pendulum stable in the upward position under the effects of friction forces and external disturbances

1.5 Objectives

The main objective for this study is to design a fuzzy sliding mode controller to swing up and stabilize the CIP system. Several objectives are set to achieve the main objective, as follows:

1- To derive third order mathematical model, that combines the Cart-Pendulum with its DC motor dynamics.
2- To design a fuzzy controller for swinging the pendulum up within the cart rail limits.

3- To design sliding mode controller surface in order to keep the pendulum and the cart in the stability position.
4- To test the proposed control algorithm using Matlab Simulink and Fuzzy logic tool box.
5- To implement the controller on a real CIP system and compare the experimental results with other linear controller techniques.

1.6 Thesis outline

The rest of thesis is organized as follows: in Chapter 2 a literature review covering former proposed swinging-up controller for CIP has been discussed. In addition, Stabilization controller (linear and nonlinear) has been surveyed. A Third order combining model for cart-pendulum system with DC motor has been derived in Chapter3. The Cart-pendulum model has been obtained based on Newton's second law of motion. The friction between the cart and its rail has been described with a nonlinear friction mode. The DC motor circuit has been modeled and linked with cart-pendulum equations in the same mathematical model.

Chapter 4 presents swinging-up and stabilization controller design. Fuzzy swing-up controller has been designed in consideration of the cart rail limits. Sliding mode stabilization controller has been introduced. Moreover, LQRC has been suggested in order to be compared with the proposed sliding mode controller. In Chapter 5, CIP combining model has been cooded in Matlab Simulink. Fuzzy swing-up controller with sliding mode stabilization controller has been tested and simulation results have been presented. Also, the

swinging-up controller with LQR stabilization controller has been performed and the results has been illustrated.

In Chapter 6, the proposed control techniques have been implemented in a real CIP system. The experimental setup has been described and the experimental results have been shown. A comparative study, between the proposed controller and LQR technique, has been conducted in Chapter 7, and the results have been discussed, and the project objectives have been evaluated. Finally, the study conclusion is presented in Chapter 8, and future work is suggested.

Chapter Two

2 Literature Review

2.1 Introduction

It is known that CIP has two sub-controllers: swinging-up and stabilization. In swing up stage, the controller is applied to swing the pendulum to the upward position under the cart rail length limits. The more effective swing-up controller takes less time and fewer numbers of swings. Once the pendulum reaches the upright position, it should be balanced by a proper stabilization controller. This controller keeps the pendulum stable at the upright position, despite friction forces and external disturbances.

For the real controller implementation, several constraints should be considered. For example, the friction force between the cart and the rail which acts as an unknown disturbance that affect the system stability. Also, there are limits for the maximum control signal and the rail length. Moreover, the actuator dynamics have to be deemed for experimental application.

In this chapter, a literature review covering CIP swinging up and stabilization controllers is presented. The swinging-up controllers review contains the main control techniques that have been introduced during the last two decades in order to solve the swing-up problem. The stabilization control review is divided into two subsections: linear techniques and nonlinear techniques. In nonlinear controller review we mainly focused on the sliding mode control which has been developed in this work. Finally, the study plan is explained based on the found gaps.

2.2 Swinging-up controllers

In literature, several Swing-up controllers have been introduced during the last two decades to swing the pendulum system to the upward position. Starting with classical methods, (Furuta et al., 1991) by using feed forward control method and (Furuta et al., 1992) that used pseudo state feedback controller to swing up Futura pendulum.

New controller for swinging-up the pendulum has been developed based on the pendulum energy, it has been known as energy control method (Åström andFuruta, 1996, 2000). In this technique, the pendulum energy (kinetic and potential) was controlled to equal the upward position energy. This method gives a direct relation between the maximum acceleration of the pendulum pivot and the number of required swing. However, the pivot velocity and position are not considered, thus makes this techniques are not applicable for CIP where the cart rail is limited. Numbers of swing-up techniques have been proposed based on the energy control principle such as, (Shiriaev et al., 2001) where variable structure control version of energy based controller has been suggested to swing up the pendulum. and (Bugeja, 2003)where swinging-up and stabilization controller based on feedback linearization and energy considerations is proposed. However none of these controllers have been tested on a real system.

A Sliding Mode Control law for swinging the pendulum up in one time without swinging motion has been proposed (M. S. Park andChwa, 2009). Simulation and experimental results show the validity for this controller for futura pendulum, where the base motion is unlimited. A new controller based on planning trajectory was proposed and implemented

on a real Futura pendulum (La Hera et al., 2009). The result shows the controller effectiveness in swining-up the system.

In (Mason et al., 2008; Mason et al., 2007), an optimal time swinging-up controller is proposed to swing-up the pendulum. In this controller, the cart acceleration is considered to be the system input. Therefore, this controller cannot be implemented easily, because of neglecting of the system actuator.

Nonlinear controller has been applied in (Wei et al., 1995), where the cart rail limits are considered. This controller needs less cart motion comparing to classical linear controllers control laws. In (Chatterjee et al., 2002), energy well swinging-up controller is designed, where the cart rail restrictions are considered. In addition, linear stabilization controller is introduced to catch the pendulum in the upright position. Simulation and experimental results show the validity for this controller. However, in the swing-up part, five different parameters should be chosen by try and error which is not simple. More simple swinging-up controller has been proposed by (Yang et al., 2009) with only two design parameters. This controller shows more simplicity in tuning the controller. However, this controller has been tested experimentally; the stabilization part has not been studied.

A simple fuzzy swinging-up controller with stabilization controller was introduced in (Muskinja andTovornik, 2006). Simulation and experimental results confirmed the effectiveness of the swinging-up controller comparing with energy control method. However, the stabilization controller does not guarantee the stability because of model linearization.

2.3 Stabilization controllers

Stabilization controllers of IP systems could be classified into two types: linear and nonlinear control techniques. In linear type, the system is approximated to linear model, where the classical control theories are applied directly. However, this kind of controller might suffer from global instability because of the model inaccuracy due to linearization. In nonlinear control techniques, controllers are designed based on the exact model without approximation. These techniques are much complicated however, the system stability is guaranteed and the system response is significantly improved compared with linear controllers.

2.3.1 Linear Stabilization controllers

Since 1960s, inverted pendulum was used to demonstrate linear control techniques such as PID (Proportional Integration Derivative) and LQR (Linear Quadratic Regulator) and Feedback Linearization (FBL) (Furuta et al., 1978; Mori et al., 1976; Sugie andFujimoto, 1994) .Generally, PID controllers are used to control SISO (Single-Input Single-Output) systems. As CIP is considered as SIMO (Single-Input Multi-Output) system, two PID should be used together to control the pendulum and the cart. In this type of controller, six parameters should be selected to carefully to control the system, so that the controller tuning quite difficult. Thus, advanced techniques like neural network are used to tune the controller (Faizan et al., 2010) (Fallahi andAzadi, 2009; Fujinaka et al., 2000; Rani et al., 2011). FBL controller has been proposed by (El-Hawwary et al., 2006). In order to improve the system stability and the disturbance rejection ability, a damping term and an adaptive fuzzy term is added. Simulation and experimental results show the validity for this controller.

Linear quadratic Regulator (LQR) control technique was also used to stabilize the pendulum system. In this scheme the pendulum system model is approximated into the linear state space form. Afterward, the feedback gains are calculated based on the minimum cost function this method shows better result and simple control scheme comparing with PID (Barya et al., 2010; Prasad et al., 2011, 2012; Wongsathan andSirima, 2009) .

In order to improve the linear controller response, LQR with nonlinear friction compensator has been proposed in (Campbell et al., 2008; D. Park et al., 2006). In these studies, nonlinear friction compensators, based on nonlinear friction models, are used to improve the steady state result. Simulation and experimental result showed the controller ability to reject some oscillation which caused by friction forces.

2.3.2 Nonlinear Stabilization controllers

In order to guarantee the system stability, nonlinear control techniques has been applied to control CIP system. In these methods, a nonlinear model is derived for the system in order to achieve better stability comparing to linear algorithms.

New Takagi-Sugeno (T-S) fuzzy model has been proposed for CIP by (Tao, Taur, Hsieh, et al., 2008). A fuzzy controller with a parallel distributed pole was designed to stabilize the system. In addition, nonlinear friction model, control signal constraints and cart rail limits were considered. Only simulation work has done to prove the controller effectiveness. Sliding mode controller was proposed in (Tao, Taur, Wang, et al., 2008) to control CIP. The system model was divided into two subsystems (cart and pendulum), sliding mode controller has been proposed for each subsystem. The controller parameters were adjusted

by an adaptive mechanism. Simulation results showed the stability for this controller under disturbances.

Decoupled sliding mode controller was proposed by(Lo andKuo, 1998). In this approach, the whole system is decoupled into two subsystems (pendulum and its cart); each one has its control target. In order to link between the two subsystems targets, an intermediate function is designed to ensure that the control signal will control both of subsystems. The fuzzy controller is added to overcome the chattering problem near the switching surface. Simulation results showed that both of the pendulum angle and the cart position converge to zero. However, this controller hasn't considered the experimental limitation, e.g., DC motor dynamics, friction and cart length restriction.

A hierarchical fuzzy sliding mode controller for CIP was introduced in (Lin andMon, 2005). In this approach, two subsystem controllers are designed for each system state and an adaptive law is used to find the controller coupling parameters. Simulation results showed the effectiveness of this controller. Neural network decoupling sliding mode controller for CIP is introduced by (Hung andChung, 2007). The coupling between the two subsystems has been done using the neural network. The results demonstrated the robustness for this controller. However, in (Hung andChung, 2007; Lin andMon, 2005) the decoupling techniques are more complicated comparing with Chang controller(Ji-Chang andYa-Hui, 1998)and experimental verification is still needed as well.

More advanced controller based on time varying sliding surface controller is proposed in (Yorgancioglu andKomurcugil, 2010). The sliding surface slope was computed by linear functions which are approximated from input-output relation of fuzzy rules. Results show improvement of the pendulum angle response in terms of speed convergence. The cart rail limits and DC motor dynamics are not considered in their study.

2.4 Study plan

In this work, a new combining model, for the cart-pendulum models and its DC motor dynamics, has been derived in third-order mathematical model. The motor control voltage is the input variable in the obtained model. This representation is applicable for the real CIP system. Friction forces between the cart and its rail are also considered in a nonlinear model.

A fuzzy swinging-up controller is designed to swing the pendulum to the upward position. Using fuzzy logic control the pendulum is swung up where the cart rail limits is considered. Once the pendulum reaches the upward position, a sliding mode controller is designed to keep the pendulum stable in the upward position. To reach the full system stability for the pendulum and the cart, an intermediate function is designed to link the cart position with the pendulum angular position. LQR controller is designed and compared with the proposed controller. The system model, controller design, simulation and experimental results are shown in subsequence sections.

Chapter Three

3 Mathematical model

3.1 Introduction

A new third order model for CIP is derived in this chapter, where the pendulum and cart dynamic are combined with the DC motor model. The main experimental limitations such as nonlinear friction force between the cart and the rail and the DC motor dynamics are considered. The derived model has the advantage of joining the mechanical system (cart and pendulum) with the electrical system (DC motor) in the same model, where the DC motor control voltage is considered as the system input.

3.2 Pendulum model

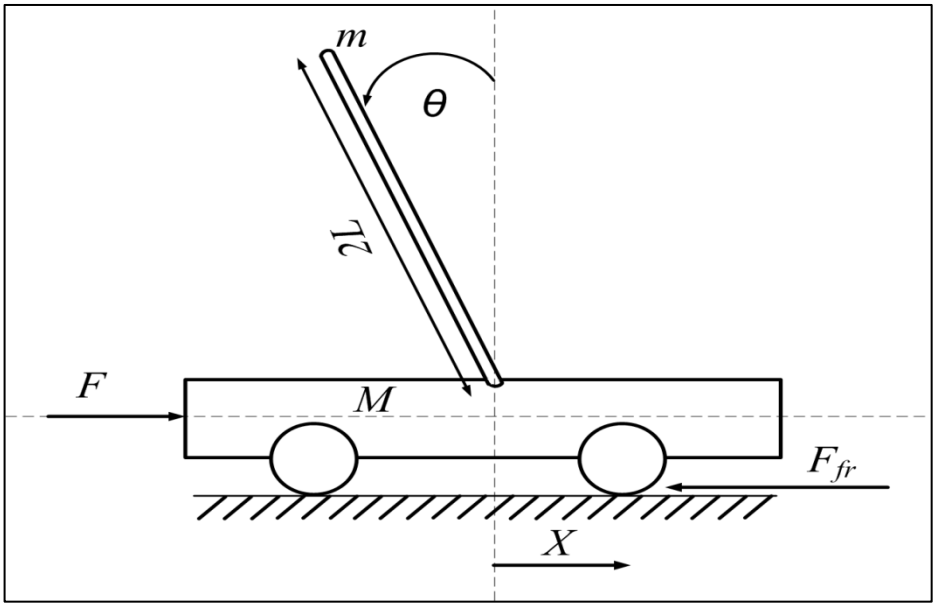

Figure 3.1: The Cart-Pendulum system

CIP has two degrees of freedom, X is the Cart displacement and θ is the pendulum angle position, as shown in Figure 3.1. The cart displacement is assumed to be positive in the right direction, and negative in the left direction. The pendulum angle is considered to be positive in CCW rotation, and negative in CW rotation. The free body diagram of the cart and the pendulum are shown in Figure 3.2 and Figure 3.3 , respectively. V is the veritical reaction force between the pendulum and the cart, H is the horizontal reaction force between the cart and the pendulum.

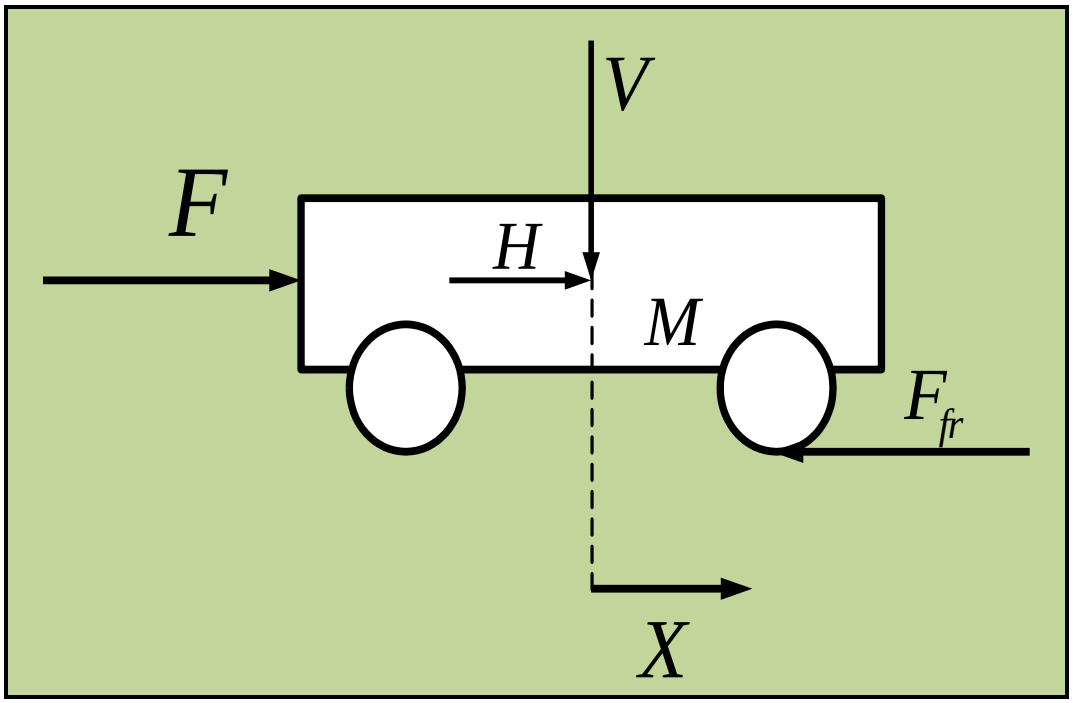

Figure 3.2: Cart free body diagram

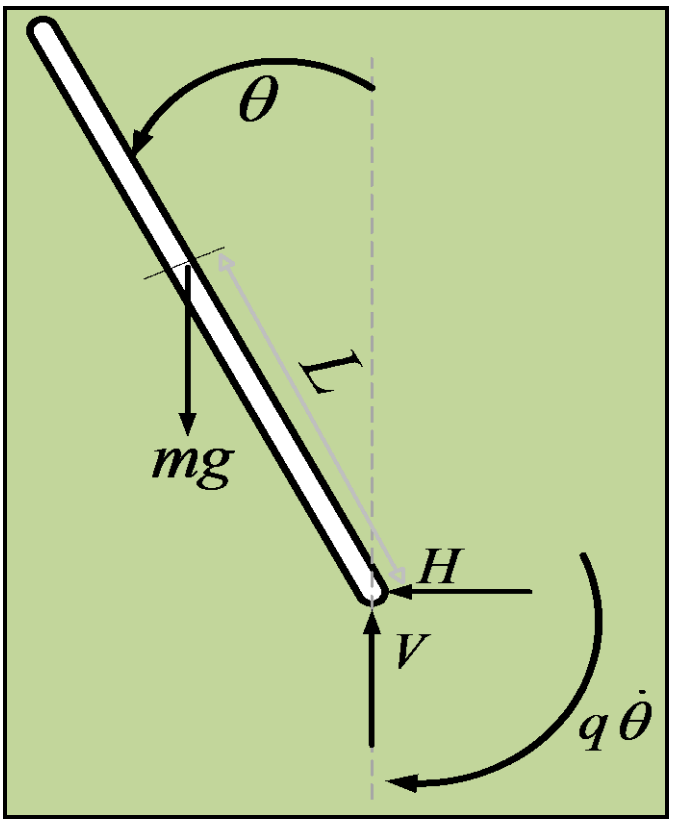

Figure 3.3: Pendulum free body diagram.

The cart mass is donated by M , m is the pendulum mass, L is the length between the pivot and the pendulum center of gravity CG, g is the acceleration of gravity, I is the pendulum mass moment of inertia with respect to its CG, F_{fr} is the friction force between the cart and the rail. q is the friction coefficient in the pendulum pivot.

Free body diagram analysis has been performed for the cart and the pendulum. For the cart free body diagram, by takingthe equlibrium of forces in the horizontal direction and applying Newton's second low of motion,the following equation is obtained:

$$M\ddot{X} = F - F_{fr} + H \qquad (3.1)$$

From the pendulum free body diagram, the summition of forces in the horizontal directions is:

$$H = m(-\ddot{X} + L\ddot{\theta}\cos\theta - L\dot{\theta}^2\sin\theta) \tag{3.2}$$

By taking forces equlibrium in the vertical direction:

$$mg - V = m(L\ddot{\theta}\sin\theta + L\dot{\theta}^2\cos\theta)$$

$$V = m\,(g - L\ddot{\theta}\sin\theta - L\dot{\theta}^2\cos\theta) \tag{3.3}$$

By summing the moments around the pendulum center of gravity:

$$I\ddot{\theta} = V L\sin\theta - H L\cos\theta - q\dot{\theta} \tag{3.4}$$

Substitute from (3.2) into (3.1), and from (3.2) and (3.3) into (3.4), the cart-pendulum equations are derived:

$$F = (M+m)\ddot{X} + F_{fr} - m(L\ddot{\theta}\cos\theta - L\dot{\theta}^2\sin\theta) \tag{3.5}$$

$$(I + mL^2)\ddot{\theta} = mgL\sin\theta + mL\ddot{X}\cos\theta - q\dot{\theta} \tag{3.6}$$

Equations (3.5) and (3.6) are the main equations of motion for the mechanical part. As it is noticed, the system input is the force *F*. This model is not applicable from practical point of view, since the DC motor is still needed to generate the force F.

3.3 Friction model

Friction is a physical phenomenon which occurs in all moving mechanical systems. It is considered as a resistive force generated between the two interacting surfaces and having a relative motion. In control systems, the friction forces have a significant effect on the system response, which might cause system instability. Steady state error and oscillations are found in the system response when the friction force is neglected. In order to eliminate such effects from the system response, the friction should be included in the system model and controller design.

Most of the earlier work, dealing with the CIP, either has applied a viscous friction model (linear) or has neglected its effects (Muskinja andTovornik, 2006). However, the friction phenomena encloses many terms such as Stribeck effects, static, Coulomb and viscous frictions (Armstrong-Hélouvry et al., 1994; Olsson et al., 1998). Thus, exponential friction model F_{fr} is chosen, to address all mentioned terms of friction, as follows:

$$F_{fr} = \begin{cases} \dot{X} \ \dfrac{F_s}{\dot{X}_d} & if \left|\dot{X}\right| \le \dot{X}_d \\ F_C + (F_S - F_C)\, e^{-\left|\dot{X}/V_S\right|^n} sgn(\dot{X}) + b\,\dot{X} & if \left|\dot{X}\right| > \dot{X}_d \end{cases} \tag{3.7}$$

Where, F_S is Static Friction force, F_C is Coulumb Friction force, $\dot{X}_{\mathrm{d}}$ is the dead zone velocities, V_S is Stribeck velocity, n is form factor, b is the viscous friction coefficient.

3.4 Dc Motor model

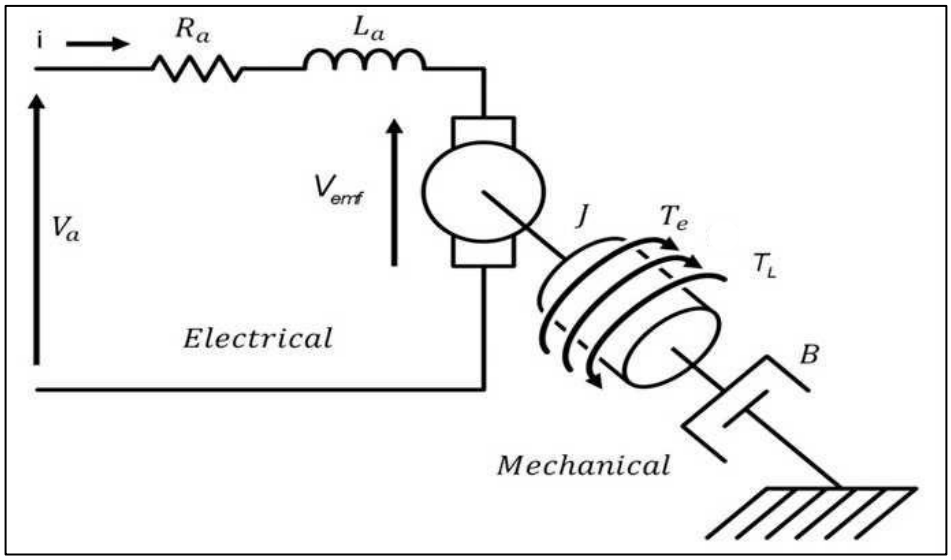

Figure 3.4: DC Motor circuit

Figure 3.4 illustrates the Dc motor Circuit, where, V_a is the armature applied voltage (Control voltage), V_{emf} is the back EMF voltage, R_a, L_a and i are the armature resistance, inductance and current, respectively. ω is the DC Motor angular velocity, T_e is the Motor electromagnetic torque, T_J is motor inertia torque, T_B is the damping torque and T_L is the motor load torque. The motor equations are

$$V_a - V_{emf} = i R_a + L_a \frac{di}{dt} \tag{3.8}$$

$$V_{emf} = K_e \omega \tag{3.9}$$

K_e is the Back EMF constant, and

$$i = \frac{T_e}{K_t} \tag{3.10}$$

K_t is the motor torque constant. The relation between the cart linear velocity and the motor

angular velocity is given by ((**3.11**).

$$\omega = \frac{\dot{X}}{r} \tag{3.11}$$

r is the motor pulley diameter. The electromagnetic torque equation will be

$$T_e = T_J + T_B + T_L \tag{3.12}$$

Where

$$T_J = J\dot{\omega} = J\frac{\ddot{X}}{r} \tag{3.13}$$

$$T_B = B\omega = B\frac{\dot{X}}{r} \tag{3.14}$$

$$T_L = Fr \tag{3.15}$$

J is the motor rotor mass moment of inertia, *B* Motor rotor damping coefficient.

3.5 Overall system model

Here, two third differential equations will be derived to describe the overall system, where the motor applied voltage V_a is the system input. By substituting from (3.13), (3.14) and (3.15) in (3.12). And from (3.12) in (3.10) we get the current equation

$$i = \frac{T_e}{K_t} = \frac{J\frac{\ddot{X}}{r} + B\frac{\dot{X}}{r} + [(M+m)\ddot{X} + F_{fr} - m(L\ddot{\theta}\cos\theta - L\dot{\theta}^2\sin\theta)]r}{K_t} \tag{3.16}$$

Taking the time derivative of the current equation, (3.17) is obtained

$$\frac{di}{dt} = \frac{[(M+m)r + \frac{J}{r}]\dddot{X} + \frac{B}{r}\ddot{X} - mLr\dddot{\theta}\cos\theta + mLr\ddot{\theta}\dot{\theta}\sin\theta + 2mLr\ddot{\theta}\dot{\theta}\sin\theta + mLr\dot{\theta}^3\cos\theta + \dot{F}_{fr}}{K_t} \tag{3.17}$$

By substituting from (3.9), (3.16) and (3.17) into (3.8), we get

$$\begin{aligned} V_a = {} & \left[[(M+m)r + \frac{J}{r}]\frac{L_a}{K_t}\right]\dddot{X} + \left[[(M+m)r + \frac{J}{r}]\frac{R_a}{K_t} + [\frac{BL_a}{rK_t}]\right]\ddot{X} \\ & - \left[[\frac{BR_a}{rK_t}] + [\frac{K_e}{r}]\right]\dot{X} - \frac{rmLR_a}{K_t}\ddot{\theta}\cos\theta + \frac{rmLR_a}{K_t}\dot{\theta}^2\sin\theta \\ & - \frac{rmLL_a}{K_t}\dddot{\theta}\cos\theta + \frac{3rmLL_a}{K_t}\dot{\theta}\ddot{\theta}\sin\theta + \frac{rmLL_a}{K_t}\dot{\theta}^3\cos\theta \\ & + \frac{R_a}{K_t}F_{fr} + \frac{L_a}{K_t}\dot{F}_{fr} \end{aligned} \tag{3.18}$$

Equation (3.18) is considered as the main overall equation, describing the system states with the applied voltage on DC motor as an input. From (3.6) we can get;

$$\ddot{X} = -g\tan\theta + \frac{(I+mL^2)}{mL\cos\theta}\ddot{\theta} + \frac{q}{mL\cos\theta}\dot{\theta} \tag{3.19}$$

$$\ddot{\theta} = \frac{mLg}{(I+mL^2)}\sin\theta + \frac{mL}{(I+mL^2)}\cos\theta\,\ddot{X} - \frac{q}{(I+mL^2)}\dot{\theta} \tag{3.20}$$

Differentiate one more time,

$$\dddot{X} = -g\,\dot{\theta} + \ddot{X}\tan\theta\,\dot{\theta} + \frac{q}{mL\cos\theta}\ddot{\theta} + \frac{(I+mL^2)}{mL\cos\theta}\dddot{\theta} \tag{3.21}$$

$$\begin{aligned}\dddot{\theta} = &\frac{mgL}{(I+mL^2)}\cos\theta\,\dot{\theta} + \frac{mL}{(I+mL^2)}\dddot{X}\cos\theta \\ &- \frac{mL}{(I+mL^2)}\ddot{X}\sin\theta\,\dot{\theta} - \frac{q}{(I+mL^2)}\ddot{\theta}\end{aligned} \tag{3.22}$$

Substituting from (3.19) and (3.21) into (3.18), we get the pendulum angle third order differential equation.

$$\dddot{\theta} = \frac{f_3\dot{\theta} - f_4\tan^2\theta\;\dot{\theta} + f_5\dfrac{\tan\theta\dot{\theta}\ddot{\theta}}{\cos\theta} + f_6\dfrac{\tan\theta\dot{\theta}^2}{\cos\theta} + f_7\dfrac{\ddot{\theta}}{\cos\theta}}{\left[f_1\cos\theta - \dfrac{f_2}{\cos\theta}\right]}$$

$$\frac{-f_8\tan\theta + f_9\dfrac{\dot{\theta}}{\cos\theta} + f_{10}\dot{X} - f_{11}\ddot{\theta}\cos\theta + f_{12}\dot{\theta}^2\sin\theta}{\left[f_1\cos\theta - \dfrac{f_2}{\cos\theta}\right]} \tag{3.23}$$

$$\frac{+f_{13}\dot{\theta}\ddot{\theta}\sin\theta + f_{14}\dot{\theta}^3\cos\theta + f_{15}F_{fr} + f_{16}\dot{F}_{fr}}{\left[f_1\cos\theta - \dfrac{f_2}{\cos\theta}\right]} - \frac{1}{\left[f_1\cos\theta - \dfrac{f_2}{\cos\theta}\right]}V_a$$

Where the values of constants $f_{1\rightarrow 16}$ are:

$$f_1 = \frac{r\, m\, L\, L_a}{K_t}\,,\quad f_2 = \frac{[(M+m)r + \frac{J}{r}]\;\; L_a\;\; [I + mL^2]}{K_t\, m\, L}\,, f_3 = \frac{[(M+m)r + \frac{J}{r}]\;\; L_a\; g}{K_t}$$

$$f_4 = \frac{[(M+m)r + \frac{J}{r}]\;\; L_a\, g}{K_t}, f_5 = \frac{[(M+m)r + \frac{J}{r}]\;\; L_a\;\; [I + mL^2]}{K_t\, m\, L},\; f_6 = \frac{[(M+m)r + \frac{J}{r}]\;\; L_a\;\; q}{K_t\, m\, L}$$

$$f_7 = \frac{[(M+m)r + \frac{J}{r}]\;\; L_a\; q \;+\; [\,[(M+m)r + \frac{J}{r}]\, R_a + [\,\frac{B\, L_a}{r}\,]\,]\,(I + mL^2)}{K_t\, m\, L}$$

$$f_8 = \Big[\,[(M+m)\, r + \frac{J}{r}]\,\frac{R_a}{K_t} + [\,\frac{B\, L_a}{r\, K_t}\,]\,\Big]\; g \qquad f_9 = \frac{\Big[\,[(M+m)r + \frac{J}{r}]\, R_a + [\,\frac{B\, L_a}{r}\,]\,\Big]\; q}{K_t\, m\, L},$$

$$f_{10} = \Big[\,[\frac{B\, R_a}{r\, K_t}] + [\frac{K_e}{r}]\,\Big],\; f_{11} = \frac{r\, m\, L\, R_a}{K_t}\,,\quad f_{12} = \frac{r\, m\, L R_a}{K_t}\; f_{13} = \frac{3 r\, m\, L\, L_a}{K_t},\; f_{14} = \frac{r\, m\, L\, L_a}{K_t}$$

$$f_{15} = \frac{R_a}{K_t},\; f_{16} = \frac{L_a}{K_t}$$

Equation (3.21) is rewritten in the form:

$$\ddot{\theta} = \alpha_1(\dot{\theta}, \theta, \dot{X}, X) + \beta_1((\dot{\theta}, \theta, \dot{X}, X)\; V_a \qquad (3.24)$$

Where,

$$\alpha_1 = \frac{f_3\dot{\theta} - f_4\tan^2\theta\ \dot{\theta} + f_5\frac{\tan\theta\dot{\theta}\ddot{\theta}}{\cos\theta} + f_6\frac{\tan\theta\dot{\theta}^2}{\cos\theta}}{[f_1\cos\theta - \frac{f_2}{\cos\theta}]}$$

$$\frac{+f_7\frac{\ddot{\theta}}{\cos\theta} - f_8\tan\theta + f_9\frac{\dot{\theta}}{\cos\theta} + f_{10}\dot{X} - f_{11}\ddot{\theta}\cos\theta}{[f_1\cos\theta - \frac{f_2}{\cos\theta}]} \qquad (3.25)$$

$$\frac{+f_{12}\dot{\theta}^2\sin\theta + f_{13}\dot{\theta}\ddot{\theta}\sin\theta + f_{14}\dot{\theta}^3\cos\theta + f_{15}F_{fr} + f_{16}\dot{F}_{fr}}{[f_1\cos\theta - \frac{f_2}{\cos\theta}]}$$

$$\beta_1 = -\frac{1}{[f_1\cos\theta - \frac{f_2}{\cos\theta}]} \qquad (3.26)$$

Similarly to get the cart position third order differential equation, substitute from (3.20) and (3.22) into (3.18)

$$\dddot{X} = \frac{-f_3'\cos^2\theta\ \dot{\theta} + f_4'\ddot{X}\sin\theta\cos\theta\ \dot{\theta} + f_5'\cos\theta\sin\theta + f_6'\cos^2\theta\ddot{X}}{[f_2'\cos^2\theta - f_1']}$$

$$\frac{+f_7'\cos\theta\dot{\theta} + f_8'\ddot{X} + f_9'\dot{X} + f_{10}'\dot{\theta}^2\sin\theta + f_{11}'\dot{\theta}\sin^2\theta + f_{12}'\dot{\theta}\sin\theta\cos\theta\ddot{X}}{[f_2'\cos^2\theta - f_1']} \qquad (3.27)$$

$$\frac{+f_{13}'\dot{\theta}^3\cos\theta + f_{14}'F_{fr} + f_{15}'\dot{F}_{fr}}{[f_2'\cos^2\theta - f_1']} - \frac{1}{[f_2'\cos^2\theta - f_1']}V_a$$

Where the values of constants $f'_{1\to15}$ are:

$$f_1' = \frac{[(M+m)r + \frac{J}{r}]\ L_a}{K_t},\ f_2' = \frac{r\,m^2L^2L_a}{(I+mL^2)K_t},\ f_3' = \frac{r\,m^2L^2L_a\,g}{(I+mL^2)K_t}$$

$$f_4' = \frac{r\,m^2L^2L_a\,g}{(I+mL^2)K_t},\ f_5' = \frac{r\,m^2L^2L_a\,q\,g}{(I+mL^2)^2\,K_t} - \frac{r\,m^2L^2R_a\,g}{(I+mL^2)K_t}$$

$$f_6' = \frac{r\,m^2L^2L_a\,q}{(I+mL^2)^2\,K_t} - \frac{r\,m^2L^2R_a}{(I+mL^2)\,K_t},\ f_7' = \frac{r\,m\,L\,L_a\,q^2}{(I+mL^2)^2\,K_t} - \frac{r\,m\,L\,R_a q}{(I+mL^2)\,K_t}$$

$$f_8' = \Big[\,[(M+m)r + \frac{J}{r}]\,\frac{R_a}{K_t} + [\,\frac{B\,L_a}{r\,K_t}\,]\Big],\quad f_9' = \Big[\,[\frac{B\,R_a}{r\,K_t}] + [\frac{K_e}{r}]\Big],$$

$$f_{10}' = \frac{r\,m\,L\,R_a}{K_t} - \frac{3r\,m\,L\,L_a q}{(I+mL^2)K_t}$$

$$f_{11}' = \frac{3r\,m^2L^2L_a\,g}{(I+mL^2)K_t},\ f_{12}' = \frac{3r\,m^2L^2L_a}{(I+mL^2)K_t},\ f_{13}' = \frac{r\,m\,L\,L_a}{K_t},\ f_{14}' = \frac{R_a}{K_t},\ f_{15}' = \frac{L_a}{K_t}$$

Equation (3.27) is rewritten in the form:

$$\ddot{X} = \alpha_2(\dot{\theta},\theta,\dot{X},X) + \beta_2(\dot{\theta},\theta,\dot{X},X)V_a \qquad (3.28)$$

Where,

$$\alpha_2 = \frac{-f_3' \cos^2\theta\ \dot{\theta} + f_4' \ddot{X} \sin\theta \cos\theta\ \dot{\theta} + f_5' \cos\theta \sin\theta}{[f_2' \cos^2\theta - f_1']}$$

$$\frac{+f_6' \cos^2\theta \ddot{X} + f_7' \cos\theta\dot{\theta} + f_8' \ddot{X} + f_9' \dot{X} + f_{10}' \dot{\theta}^2 \sin\theta}{[f_2' \cos^2\theta - f_1']} \qquad (3.29)$$

$$\frac{+f_{11}' \dot{\theta} \sin^2\theta + f_{12}' \dot{\theta} \sin\theta \cos\theta \ddot{X} + f_{13}' \dot{\theta}^3 \cos\theta + f_{14}' F_{fr} + f_{15}' \dot{F}_{fr}}{[f_2' \cos^2\theta - f_1']}$$

$$\beta_2 = -\frac{1}{[f_2' \cos^2\theta - f_1']} V_a \qquad (3.30)$$

Chapter Four

4 Methodology

4.1 Introduction

Methodology of Swinging-up and stabilization control is discussed in this chapter. For the pendulum swinging-up, fuzzy logic controller is designed to achieve the task in consideration of the cart rail limits. After reaching the upward position, SMC is developed to guarantee the system stability. Linear control technique (LQRC) is designed, in order to be compared with the proposed SMC. The controller schematic diagram is shown in Figure4.1.

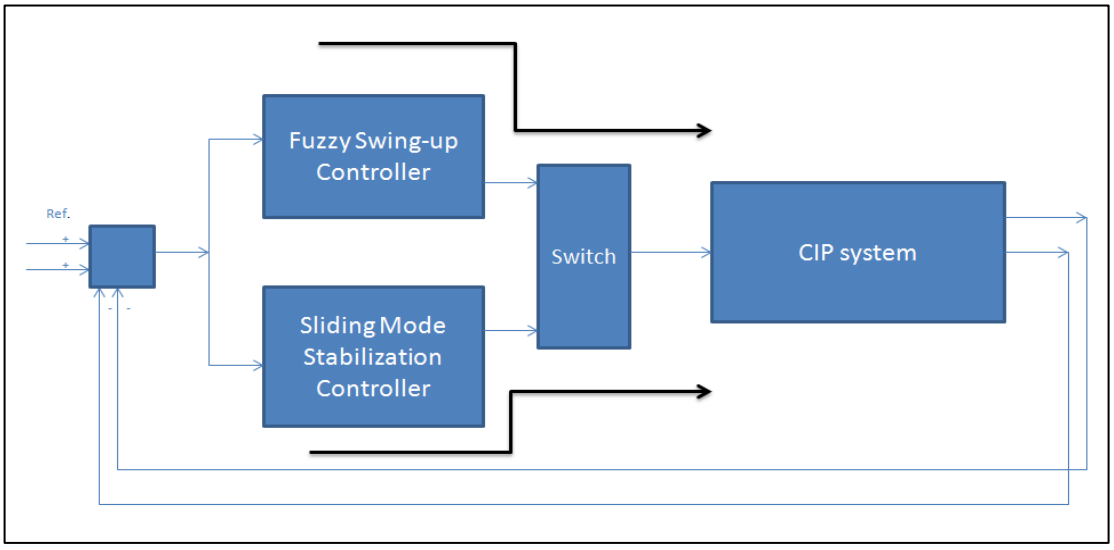

Figure4.1: schematic diagram for Swing up with stabilization controller.

4.2 Fuzzy swing-up controller

The main idea of the fuzzy swinging–up controller is based on the pendulum energy, which equals the summation of its kinetic and potential energies(Åström andFuruta, 2000). By

controlling this energy, and raise it to equal the upward position energy, the pendulum could be swung-up. The pendulum energy E is given by

$$E = I_P \dot{\theta}^2 + m g L \cos\theta \qquad (4.1)$$

Where, I_P is the pendulum mass moment of inertia around the pivot point. According to (4.1), the pendulum energy depends on the pendulum angle and the pendulum angular velocity. In other words, the pendulum energy can be increased by controlling the variables θ and $\dot{\theta}$. The cart rail limit should be also considered in swinging-up thus, for the fuzzy controller, three input variables are chosen: the pendulum angle θ, the pendulum angular velocity $\dot{\theta}$ and the cart displacement X. The DC motor control voltage V_a is the output variable.

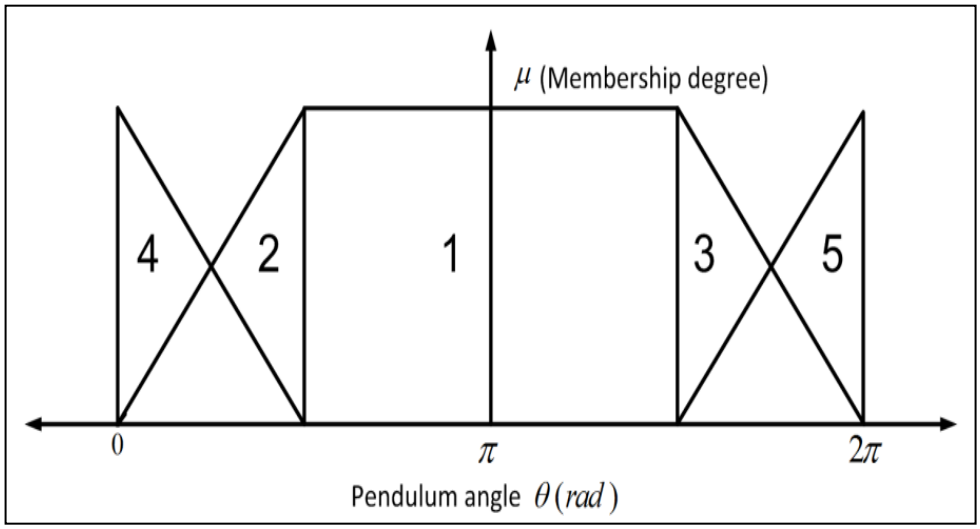

Figure 4.2: Membership functions of the pendulum angle.

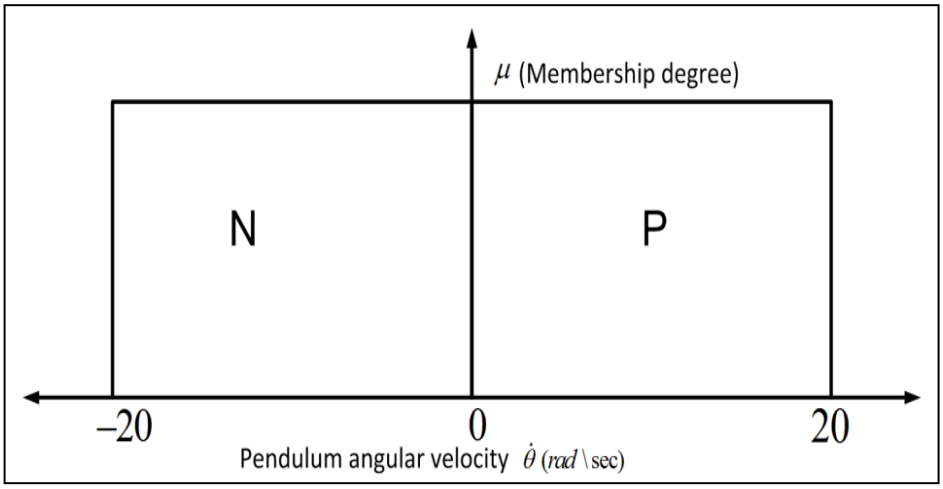

Figure 4.3: Membership functions of the pendulum angular velocity.

As it is shown in Figure 4.2, five membership functions (1, 2, 3, 4 and5) are chosen for the pendulum angle. Note that the rectangular membership function (1) represents the pendulum angle if ($\pi/2 \leq \theta < 3\pi/2$), where, the accurate pendulum angle measurement is not required. The other four membership functions are chosen to be in a triangular shape because they are located near to the upward position, where more accurate measurement is needed. In Figure 4.3, the pendulum angular velocity is represented by two membership functions N (counter clock wise) and P (clock wise) as illustrated. The cart displacement is represented by two triangular (P and N) and one trapezoidal (Zero) membership functions (Zero) as shown in Figure 4.4. For the output control voltage, seven singleton membership functions are selected in Figure 4.5, to represent the applied control voltage on the DC motor. The singleton membership functions positions are chosen to minimize the swinging-up time.

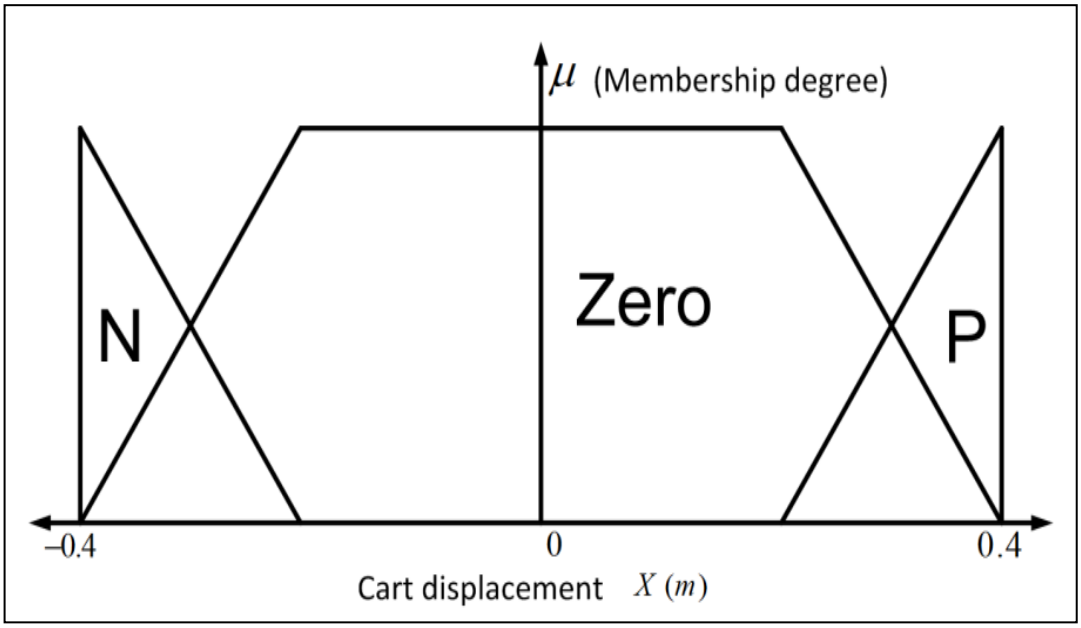

Figure 4.4: Membership functions of the cart position.

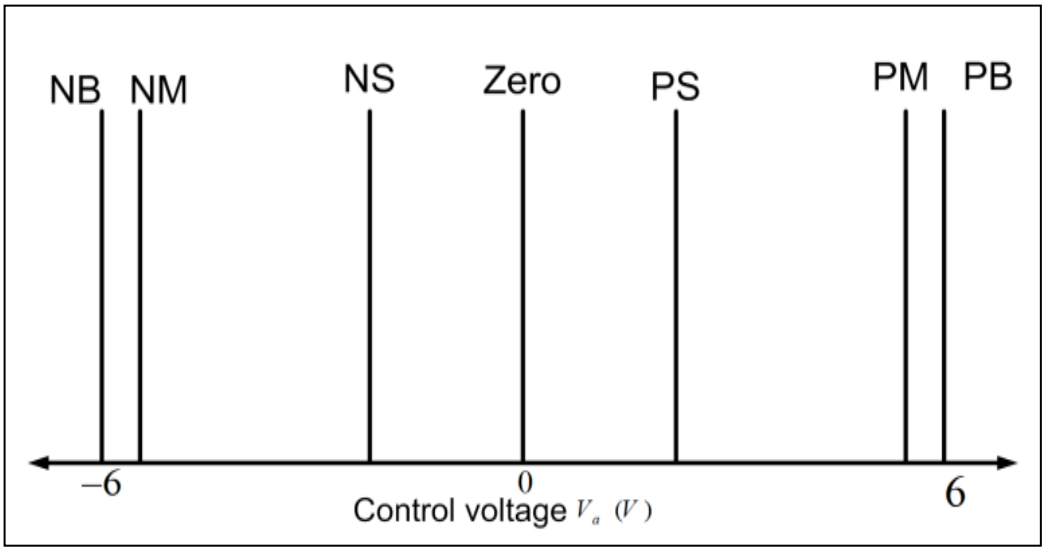

Figure 4.5 : Membership functions of the output control voltage.

The swing-up controller is designed based on 30 fuzzy rules. The rules consequents are chosen to increase the pendulum energy to reach the upward position energy. During the swinging-up, the cart rail limitation should be considered. Each three rules are designed at the same Pendulum angle θ and angular velocity $\dot{\theta}$, with consideration of the cart position.

For instance, if the pendulum angle is 1 and the pendulum angular velocity is N, the three rules are developed as follows: First, without consideration of the cart limits, the logical swing-up control action should be PB. Then, the cart position membership functions (N,P and Zero) will be considered to form the three rules, for each rule θ and $\dot{\theta}$ are constant (1 and N, respectively).

Rule1:

If θ is 1 and $\dot{\theta}$ is N and X is P, then Va(swing-up) is Zero.

It means that the pendulum is located in the downward half cycle ($\pi/2 \leq \theta < 3\pi/2$) and it rotates in CW direction. As it is mentioned above, the logical swing-up control decision should be PB. Since the cart is located at the positive side of the rail (X is P).Thus, In order to keep the cart within the limits, and the rule consequent should be Va(swing-up) is Zero.

Rule 2:

If θ is 1 and $\dot{\theta}$ is N and X is Zero, then Va(swing-up) is PM.

For this rule the cart is located in the middle of the rail (X is Zero). Thus, the control action will be chosen to move the cart in the positive direction, but with a medium force, and the rule consequent will be Va(swing-up) is PM.

Rule 3:

If θ is 1 and $\dot{\theta}$ is N and X is N, then Va(swing-up) is PB.

Because the cart is located at the rail negative side (X is N), the the rule consequent will be kept Va(swing-up) is PB

The rest 27 rules are chosen with the same procedures. This controller allows the pendulum to reach the upward position while the cart remains within the restricted limits. The fuzzy swing-up rules are as follows:

Rule 4: If θ is 1 and $\dot{\theta}$ is P and X is P, then Va(swing-up) is NB

Rule 5: If θ is 1 and $\dot{\theta}$ is P and X is Zero, then Va(swing-up) is NM

Rule 6: If θ is 1 and $\dot{\theta}$ is P and X is N, then Va(swing-up) is Zero

Rule 7: If θ is 2 and $\dot{\theta}$ is N and X is P, then Va(swing-up) is NB

Rule 8 : If θ is 2 and $\dot{\theta}$ is N and X is Zero, then Va(swing-up) is NM

Rule 9: If θ is 2 and $\dot{\theta}$ is N and X is N, then Va(swing-up) is Zero

Rule 10: If θ is 2 and $\dot{\theta}$ is P and X is P, then Va(swing-up) is Zero

Rule 11 : If θ is 2 and $\dot{\theta}$ is P and X is Zero, then Va(swing-up) is PM

Rule 12: If θ is 2 and $\dot{\theta}$ is P and X is N, then Va(swing-up) is PB

Rule 13: If θ is 3 and $\dot{\theta}$ is N and X is P, then Va(swing-up) is NB

Rule 14: If θ is 3 and $\dot{\theta}$ is N and X is Zero, then Va(swing-up) is NM

Rule 15: If θ is 3 and $\dot{\theta}$ is N and X is N, then Va(swing-up) is Zero

Rule 16: If θ is 3 and $\dot{\theta}$ is P and X is P, then Va(swing-up) is Zero

Rule 17: If θ is 3 and $\dot{\theta}$ is P and X is Zero, then Va(swing-up) is PM

Rule 18: If θ is 3 and θ̇ is P and X is N, then Va(swing-up) is PB

Rule 19: If θ is 4 and θ̇ is N and X is P, then Va(swing-up) is NM

Rule 20: If θ is 4 and θ̇ is N and X is Zero, then Va(swing-up) is NS

Rule 21: If θ is 4 and θ̇ is N and X is N, then Va(swing-up) is Zero

Rule 22: If θ is 4 and θ̇ is P and X is P, then Va(swing-up) is Zero

Rule 23: If θ is 4 and θ̇ is P and X is Zero, then Va(swing-up) is PS

Rule 24: If θ is 4 and θ̇ is P and X is N, then Va(swing-up) is PM

Rule 25: If θ is 5 and θ̇ is N and X is P, then Va(swing-up) is NM

Rule 26: If θ is 5 and θ̇ is N and X is Zero, then Va(swing-up) is NS

Rule 27: If θ is 5 and θ̇ is N and X is N, then Va(swing-up) is Zero

Rule 28: If θ is 5 and θ̇ is P and X is P, then Va(swing-up) is Zero

Rule 29: If θ is 5 and θ̇ is P and X is Zero, then Va(swing-up) is PS

Rule 30: If θ is 5 and θ̇ is P and X is N, then Va(swing-up) is PM

Note, the swing-up time could be controlled by selecting the output voltage (V_a) membership functions. In the real application, the swing-up time also depends on the DC motor maximum voltage.

The control output value has been utilized by center of gravity defuzzification method. The fuzzy controller uses the following equation has been used to obtain the real control output

$$CoA = \frac{\int_{x_{min}}^{x_{max}} \mu(x).x \; dx}{\int_{x_{min}}^{x_{max}} \mu(x) \; dx}$$

Where CoA is the center of area which represents the control output, x is value of linguistic variable, x_{max} and x_{min} are the linguistic variable range. μ(x) is the variable membership.

4.3 Sliding Mode stabilization controller

Sliding Mode Controller is designed based on the third order derived mode. From the system model in (3.24) and (3.28), and if $D_1$and D_2 are bounded external disturbances, the entire system model will have the following form

$$\dddot{\theta} = \alpha_1 + \beta_1 V_a + D_1 \tag{4.2}$$

$$\dddot{X} = \alpha_2 + \beta_2 V_a + D_2 \tag{4.3}$$

Where, α_1 and β_1 are nonlinear functions of the system states θ, X, $\dot{\theta}$, $\dot{X}$ and $\ddot{\theta}$. α_2 and β_2 are functions of θ, X, $\dot{\theta}$, $\dot{X}$ and $\ddot{X}$. The control law is designed based on the sliding surface. The general equation of the sliding surface S is (Bartoszewicz andNowacka-Leverton, 2010; Palm et al., 1997)

$$S(x,t) = \left(\frac{d}{dt} + C\right)^{n-1} . x \tag{4.4}$$

Where x is the system sate, n is the system order and C is a constant value. In this case (CIP) the system states are θ, $\dot{\theta}$, $\ddot{\theta}$, X, $\dot{X}$ and $\ddot{X}$. Thus, two sliding surfaces, S_1 for the pendulum subsystem and S_2 for the cart subsystem, are considered. Where

$$S_1 = C_1^{\,2}\theta + 2C_1\dot{\theta} + \ddot{\theta} \tag{4.5}$$

$$S_2 = C_2^{\,2} X + 2C_2 \dot{X} + \ddot{X} \tag{4.6}$$

C_1 and C_2 are positive constants. Sliding surfaces S_1 andS_2 are constructed based on the constants C_1 and C_2. Appropriate selection of these constants values will achieve the desired response.

The control law is designed based on the sliding surfaces. Since only one control action is available, the Pendulum angle will be considered as primary control target and the cart position is the secondary target. Initially, the controller is designed to achieve the primary target where $S_1 = 0$. An intermediate function is used to link between the secondary and primary targets. This function will achieve the cart subsystem stability if the pendulum stability is reached. The control law is designed based on Lyapunov like function V

$$V = \frac{1}{2} S_1^{\,2} \tag{4.7}$$

As it is known from sliding mode theorem, in order to achieve the system stability the control law must match the following reaching condition

$$\dot{V} = \dot{S_1} S_1 \le \eta \left| S_1 \right| \tag{4.8}$$

Where $\eta > 0$, this condition ensures that the system will be driven into the sliding mode. The control law will be derived as follow, from (4.8)

$$\dot{S_1}.\mathrm{sgn}(S_1) \le \eta \tag{4.9}$$

Taking the first derivative for (4.5)

$$\dot{S_1} = (C_1^{\,2} \dot{\theta} + 2C_1 \ddot{\theta} + \dddot{\theta}) \tag{4.10}$$

Substituting with (4.10) in (4.9)

$$(C_1{}^2\dot{\theta} + 2C_1\ddot{\theta} + \alpha_1 + \beta_1 V_a + D_1).\mathrm{sgn}(S_1) \le \eta \qquad (4.11)$$

$$(C_1{}^2\dot{\theta} + 2C_1\ddot{\theta} + \alpha_1 + D_1).\mathrm{sgn}(S_1) + \beta_1 V_a.\mathrm{sgn}(S_1) \le \eta \qquad (4.12)$$

$$(\frac{C_1{}^2\dot{\theta} + 2C_1\ddot{\theta} + \alpha_1 + D_1}{\beta_1}).\mathrm{sgn}(S_1\beta_1) + V_a.\mathrm{sgn}(S_1\beta_1) \le \frac{\eta}{|\beta_1|} \qquad (4.13)$$

From (4.13), the control law could be written in form

$$V_{a(stablize)} = \frac{-C_1{}^2\dot{\theta} - 2C_1\ddot{\theta} - \alpha_1}{\beta_1} - K\ \mathrm{sgn}(S_1\beta_1) \qquad (4.14)$$

Where

$$K \ge \frac{D_1 + \eta}{|\beta_1|}$$

The first term of the control law is estimated from the system model, and it will be donated as $\hat{V}a(stabilize)$, where

$$\hat{V}_{a(stablize)} = \frac{-C_1{}^2\dot{\theta} - 2C_1\ddot{\theta} - \alpha_1}{\beta_1}$$

This form of the control signal guarantee the stability for the pendulum subsystem since the reaching condition is achieved and the sliding motion will occur. The control action V_a , as it is shown in (4.14), has a high-frequencies switching because of the *Sgn* function. To overcome this problem, a boundary layer will be formed by replacing *Sgn* function with Sat function as follows,

$$V_a = \hat{V}_a - K\ Sat(\frac{S_1 \beta_1}{\phi}),\ where \quad \phi > 0 \tag{4.15}$$

Where

$$Sat(\frac{S_1 \beta_1}{\phi}) = \begin{cases} Sgn\ \frac{S_1 \beta_1}{\phi}, & if \left|\frac{S_1 \beta_1}{\phi}\right| \geq 1 \\ \frac{S_1 \beta_1}{\phi}, & if \left|\frac{S_1 \beta_1}{\phi}\right| < 1 \end{cases} \tag{4.16}$$

This kind of control will be capable of rejecting all the high-frequencies and solve the chattering problem.

The control law in equation (4.15) can only guarantee the pendulum angle stability. The control objective is to move the pendulum and the cart subsystems to the sliding surfaces S_1 and S_2, respectively, where the overall system stability could be achieved. In order to do that, an intermediate function *Z* has been introduced to link between the two subsystems sliding surfaces S_1 and S_2. The function *Z* design is introduced as follows:

First, the first sliding surface will be reformed to be

$$S_1 = C_1^{\ 2}(\theta - Z) + 2C_1\dot{\theta} + \ddot{\theta} \tag{4.17}$$

Where, Z is a function of S_2 which means that the sliding surface S_2 was incorporated into the sliding surface S_1 through Z function. The new sliding surface has changed the control target from $\theta=0$, $\dot{\theta}=0$ and $\ddot{\theta}=0$ to $\theta=Z$, $\dot{\theta}=0$ and $\ddot{\theta}=0$. The objective ($S2 = 0$) is now embedded in the main control target through the variable Z which is defined

$$Z = sat(\frac{S_2}{\phi_z}).Z_U \qquad (4.18)$$

Where, Z_U is the upper limit of the function; Φ_Z is the function boundary layer. Z is abounded oscillatory function decays to zero. When Z reach zero, S_1 will be zero according to (4.17). (Yorgancioglu andKomurcugil, 2010).

In order to prove that Z is a decaying function, from equation (4.17), if we defined θ as x_1, $\dot{\theta}$ as x_2 and $\ddot{\theta}$ as x_3. The controller guarantees that the pendulum subsystem moves towards the sliding surface $S_1=0$. Equation (4.17) could be written in the form:

$$S_1 = C_1^{\,2}(x_1 - Z) + 2C_1 x_2 + x_3 = 0$$

By taking the second derivative:

$$\ddot{S}_1 = C_1^{\,2}(\ddot{x}_1 - \ddot{Z}) + 2C_1 \ddot{x}_2 + \ddot{x}_3 = 0$$

$$\ddot{S}_1 = C_1^{\,2}(\dot{x}_3 - \ddot{Z}) + 2C_1 \dot{x}_3 + \ddot{x}_3 = 0$$

The equation could be rearranged to be

$$\ddot{x}_3 + 2C_1\dot{x}_3 + C_1^2 x_3 = C_1^2 \ddot{Z}$$

This considered as a linear nonhomogenous second order differential equation. The general solution for x_3 will be

$$x_3(t) = \left[x_3(0) + \left[\dot{x}_3(0) + C_1 x_3(0)\right]t\right]e^{-C_1 t} + C_1^2 \int_0^t \left[\int_0^t e^{-C_1 t}\ddot{Z}(\tau)d\tau\right]dt$$

Where $x_3(0)$ and $\dot{x}_3(0)$ are the initial conditions (at $t=0$).

The first term in the right side is the complementary solution which comes from solving the homogenous part, whereas the second term is the particular solution which comes by solving the nonhmogeneous part. In the steady state $x_3=0$, which is could be achieved only if the second term in the right side converges to zero. That will happen if only Z decays to zero.

4.4 LQR stabilization controller

LQR control technique is widely used for linear control applications. For CIP, many LQR controllers are designed based on the linearized system model. A six order linear model (two third order linear equation) is expected after linearizing the system equations (3.24) and (3.28)(Elsayed et al., 2013).However, for comparison purposes, and by neglecting the motor induction, we derived a forth order CIP model (two second order linear equations) like the derived models in (Chatterjee, et al., 2002; Muskinja andTovornik, 2006).

From equations (3.24) and (3.28) and by neglecting the motor inductance ($L_a=0$) and linearizing the system equation around the upward equilibrium point where $(\theta=0)$. If the pendulum was assume to move only few degrees around the upward position, where $\cos\theta=0$, $\sin\theta=\theta$ and $\dot{\theta}\theta=0$. Equations (3.24) and (3.28) will have the following forms:

$$\ddot{\theta}=(-g_6/g_5)\dot{X}+(-g_7/g_5)\theta+(g_8/g_5)\dot{\theta}+(1/g_5)V_a \quad (4.19)$$

$$\ddot{X}=(-g_2/g_1)\dot{X}+(-g_3/g_1)\theta+(g_4/g_1)\dot{\theta}+(1/g_1)V_a \quad (4.20)$$

Where

$$g_1=[R_a r/K_m][(M+m)-(m^2L^2/(I+mL^2))] \ , \ g_2=[(R_a r b/K_m)+(K_e/r)]$$

$$g_3=[(R_a r m^2 L^2 g)\backslash(K_m(I+mL^2))], \ g_4=[(R_a r m L q)\backslash(K_m(I+mL^2))]$$

$$g_5=[R_a r/K_m][(mL)-((m+M)(I+mL^2)/(mL))] \ , \ g_6=[(R_a r b/K_m)+(K_e/r)]$$

$$g_7=[R_a r g(M+m)]/[K_m], \ g_8=[R_a r q(M+m)]/[m L K_m]$$

Equations (4.19) and (4.20) are the overall system linear equation. For designing LQR controller, the system equations should be in the state space form. If the system states vector is $x=[X\ \dot{X}\ \theta\ \dot{\theta}]$, the general state-space form is

$$\dot{x} = Ax + Bu \tag{4.21}$$

Where, x is state matrix (1x4), u control signal matrix (1x1), A is state parameters matrix (4x4), B is control signal parameters matrix (1x4). Since only one control action (DC motor voltage) is available, $u = Va$. The equivalent state-space linearized system equation is

$$\begin{pmatrix} \dot{X} \\ \ddot{X} \\ \dot{\theta} \\ \ddot{\theta} \end{pmatrix} = \begin{pmatrix} 0 & 1 & 0 & 0 \\ 0 & (-g_2/g_1) & (-g_3/g_1) & (g_4/g_1) \\ 0 & 0 & 0 & 1 \\ 0 & (-g_6/g_5) & (-g_7/g_5) & (g_8/g_5) \end{pmatrix} \begin{pmatrix} X \\ \dot{X} \\ \theta \\ \dot{\theta} \end{pmatrix} + \begin{pmatrix} 0 \\ (1/g_1) \\ 0 \\ (1/g_5) \end{pmatrix} V_a \tag{4.22}$$

From LQR theory, the following sate feedback control law is applied.

$$u = V_a = -K_L x \tag{4.23}$$

Where K is the optimal feedback gain matrix required to get a minimum performance index J

$$J = \int_0^\infty (x^T Q x + u^T R u)\ dt \tag{4.24}$$

Where Q and R are a real symmetric matrices which are chosen by the designer. The gain matrix K_L is calculated by solving Reduced-matrix Riccati equation (4.25), after obtaining matrix P.

$$A^T P + PA - PBR^{-1}B^T P + Q = 0 \tag{4.25}$$

Where P is an intermediate matrix used to calculate the gain matrix K (Ogata, 2002)

$$K_L = R^{-1} B^T P \tag{4.26}$$

The controller parameter *Q* should be carefully chosen based on the states priority. Form a control point of view, the pendulum angle is much more important than the cart position *X*. Therefore, a bigger value should be chosen for the angle element in *Q* matrix. Selection of *R* matrix value depends on the control signal constrains. Based on the values of *Q* and *R*, the feedback gain matrix K_L is obtained.

4.5 Switching between swinging-up and stabilization control

In order to switch between the swinging-up and stabilization controllers, one-move switch is developed. This switch ensures the fuzzy swinging-up controller will be activated only one time. Once the pendulum reaches that upward point, the stabilization controller will be activated permanently. The switch output (Va) could be represented as follows

$$V_a = \begin{cases} V_{a(swing-up)} & if\ (0 < \theta < 2\pi),\ and\ (N < 1) \\ V_{a(stablize)} & if\ (\theta \geq 2\pi\ or\ \theta \leq 0),or\ (N \geq 1) \end{cases}$$

Where, N is an integer counter which counts the numbers of the upward position, at (θ = 0).

Chapter Five

5 Simulation results

5.1 Introduction

CIP system dynamics, given by the equations (3.24) and (3.28), have been solved and simulated using MATLAB Simulink. In cooperation with Fuzzy Logic toolbox, the fuzzy swinging-up controller is designed applied to swing the pendulum to the upward position. Two stabilization control (sliding mode and linear quadratic regulator) schemes are implemented and compared. Both controllers (SMC and LQRC) are tested in corporation with the fuzzy controller in the swinging–up phase. For testing purpose, nonlinear friction force between the cart and the rail is considered according to equation (**3.7**). This force is acting as an external disturbance on the controller. The cart rail limit is $\pm 0.4m$ and the motor saturation voltage is ±6 Volt. All CIP parameters and friction forces coefficients are listed in Table 5.1. The controller parameters, for SMC and LQRC, have been chosen to achieve fast response. DC motor saturation voltage has been also considered in the controller parameters selection. For SMC, the controller parameters are chosen to be $C_1=5.5,\ C2=3.1,\ K=15,\ \Phi = 8x10^4,\ \Phi_z = 19$ and $Z_u=0.98$ .and for LQRC the selected parameters are $R=diag\ [400\ 1\ 2500\ 1],\ Q= 4$ and the generated feedback gain vector K_L= [-10 -12.9 90.5 17.4].

Table 5.1: system parameters

Parameter	Value	Unit
M	0.882	kg
m	0.32	kg
L	0.3302	m
I	7.88×10^{-8}	$kg.m^2$
g	9.8	m/s^2
q	0.0001	N.s/rad
L_a	0.18×10^{-3}	H
R_a	2.6	Ohm
J	3.9×10^{-7}	$kg.m^2$
B	8×10^{-7}	N.m.s/rad
K_t	0.00676	N.m/A
K_e	0.00676	V.s/rad
r	6.35×10^{-3}	m
F_s	0.1	N
F_c	0.08	N
V_s	0.1	m/s
b	1.3	N.s/m
n	4	-
$\dot{X}_d$	0.05	m/s

5.2 Fuzzy swinging-up with SMC stabilization

Pendulum angle response for fuzzy swing-up with SMC is shown in Figure 5.1. It is seen that the pendulum is swung-up from downward position, where $\theta=\pi$ *rad*, into the upward position, where $\theta=0$. The pendulum is swung up within 6 seconds before the controller is switched to activate the SMC. The figure shows the effectiveness of the SMC to stabilize the pendulum, in spite of nonlinear friction forces. The cart displacement response is shown in Figure 5.2. As it is noticed, the cart starts from the rail edge, where $x= 0.4$ *m* , and it is kept within the rail limits before it is driven to the stability position . Figure 5.3 shows the control signal response, where it decayed into zero.

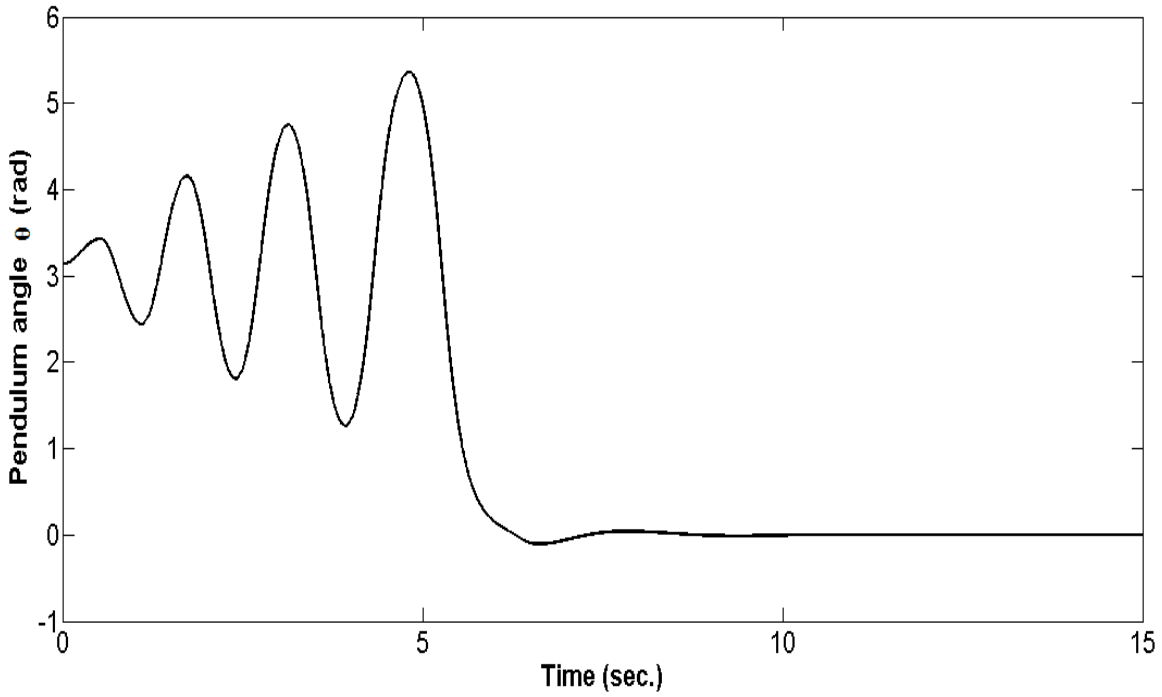

Figure 5.1: Pendulum angular position response for fuzzy swing-up with SMC.

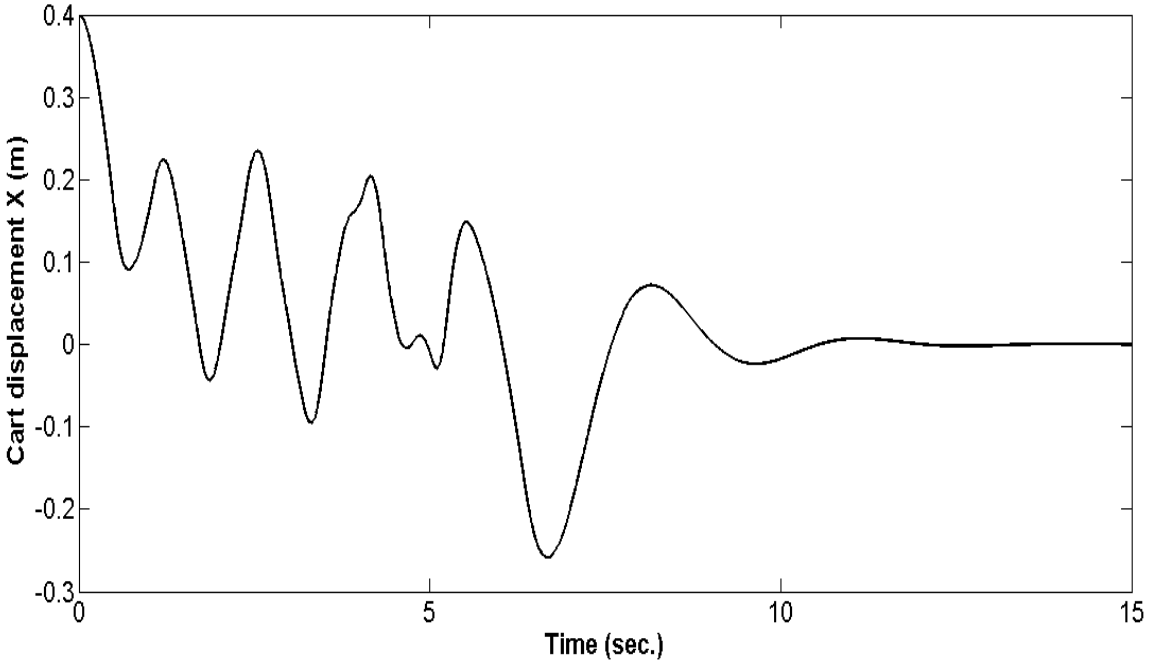

Figure 5.2: Cart position response for fuzzy swing-up with SMC.

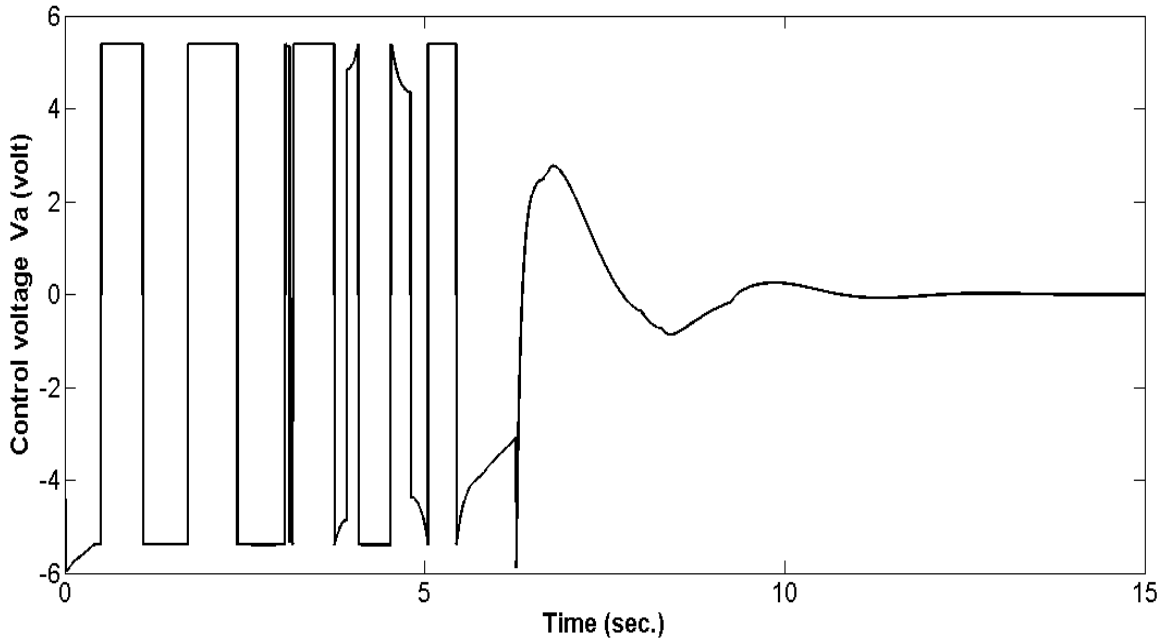

Figure 5.3: Control voltage response for fuzzy swing-up with SMC.

5.3 Fuzzy swinging up with LQR stabilization controller

Pendulum angular position response under fuzzy Swing-up together with LQRC is shown in

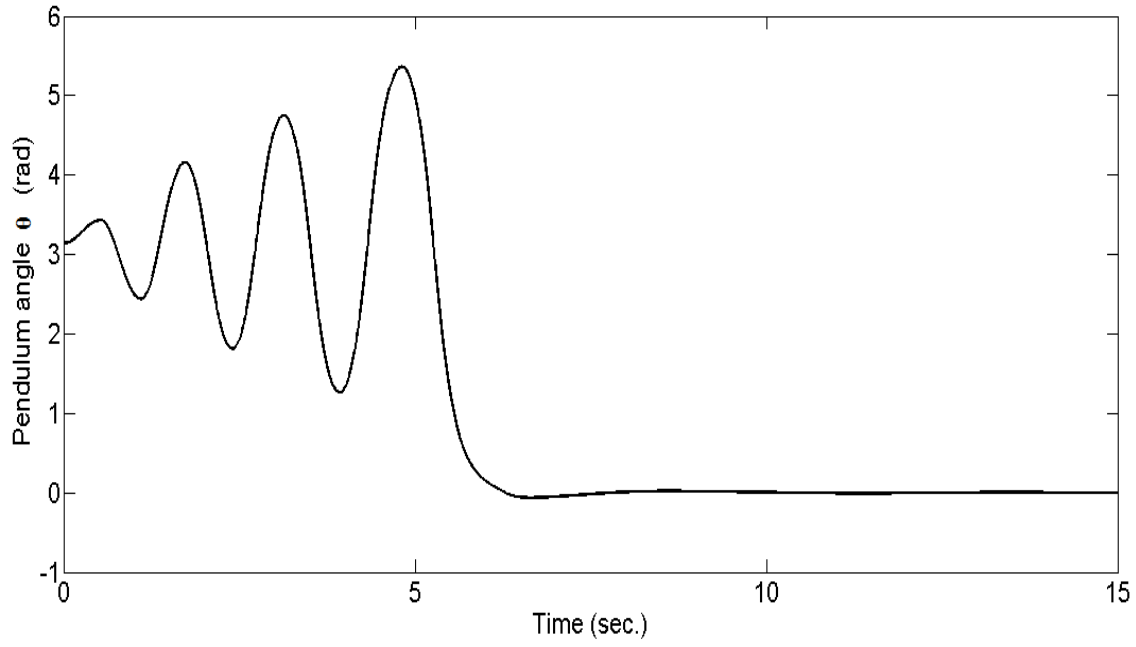

Figure **5.4**. It is could be seen that the pendulum is swung up within 6 seconds before it is balanced in the upward position. The cart response is shown in Figure 5.5, where some oscillations could be noticed in the steady state response. Figure5.6 illustrates the control signal curve, where the system doesn't achieve the stability within the simulation time. Due to friction uncertainties and system nonlinearity, LQRC could not achieve the full stability for CIP.

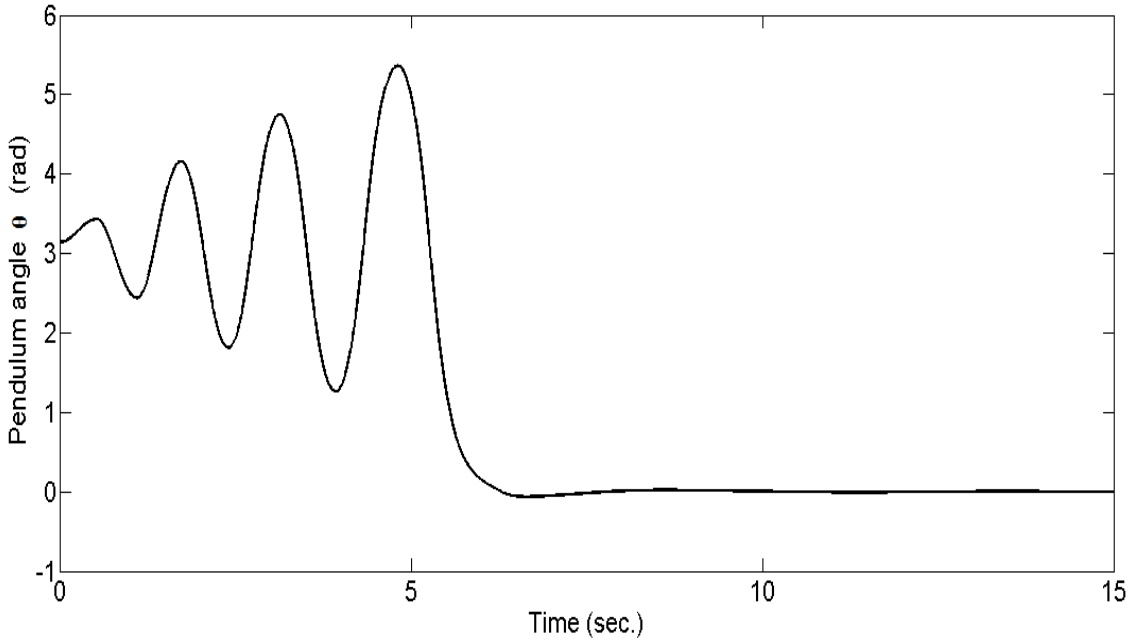

Figure 5.4: Pendulum angular position response for fuzzy swing-up with LQRC.

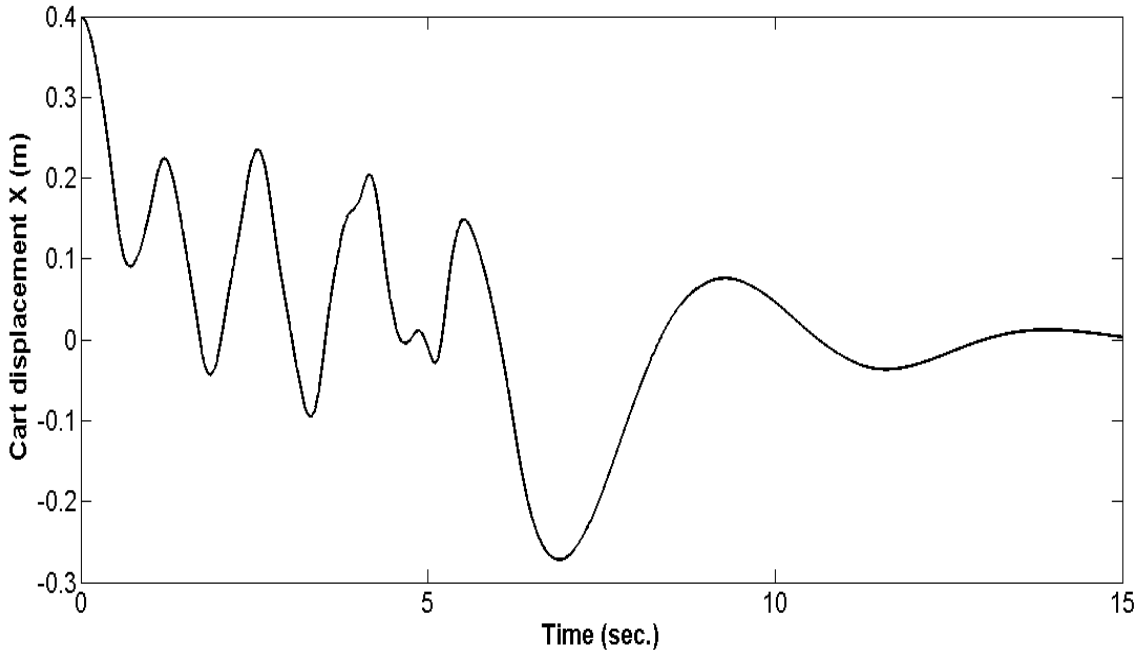

Figure 5.5: Cart position response for fuzzy swing-up with LQRC.

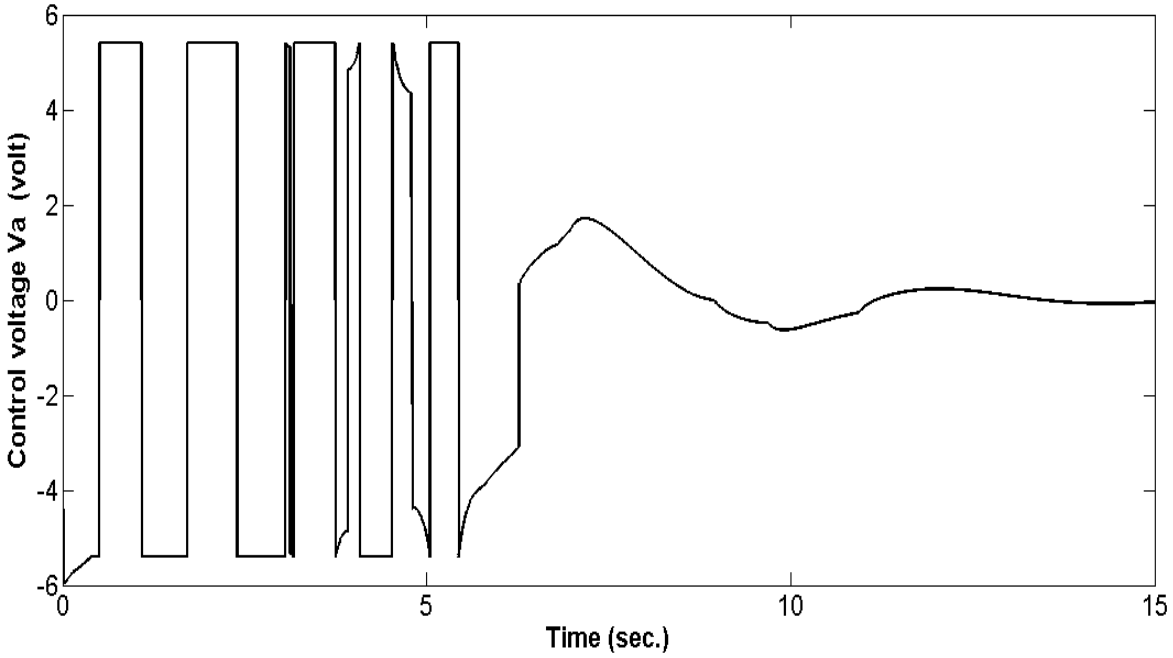

Figure5.6 : Control voltage response for fuzzy swing-up with LQRC.

Chapter Six

6 Experimental results

6.1 Introduction

Simulation results have shown the proposed SMC validity to stabilize CIP under the friction forces effects. Simulation might not be enough to prove the controller effectiveness. Since there are many several physical parameters could not considered in the dynamic model e.g., backlash effects between the pinion of the DC motor and the rack, also the air drag force that acting on the pendulum motion, wear and viscoelastic deformation in the pinion and the temperature change. In the experimental work all theses limitation and the friction force are considered as system uncertainties. In this chapter, the proposed SMC is tested and compared with LQR experimentally.

6.2 Experimental setup

6.2.1 Electro- mechanical setup

The experimental work has been performed with CIP model IP02 supplied by Quanser Limited, see Figure 6.1. The electromechanical setup consists of the cart-pendulum mechanical setup, DC motor and two incremental encoders. The encoders are used for sensing the pendulum angular position and the cart position with a resolution of 0.0015 rad/count and 2.275×10^{-5} m/count, respectively. The cart slides on a stainless steel rod

using a linear bearing and it is driven by the DC motor via rack and pinion mechanism, as it is shown in Figure 6.2.

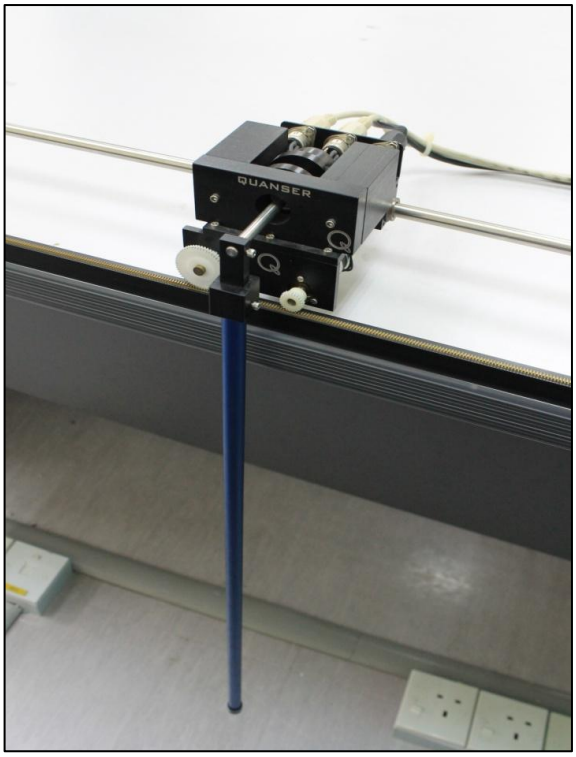

Figure 6.1: CIP model IP02

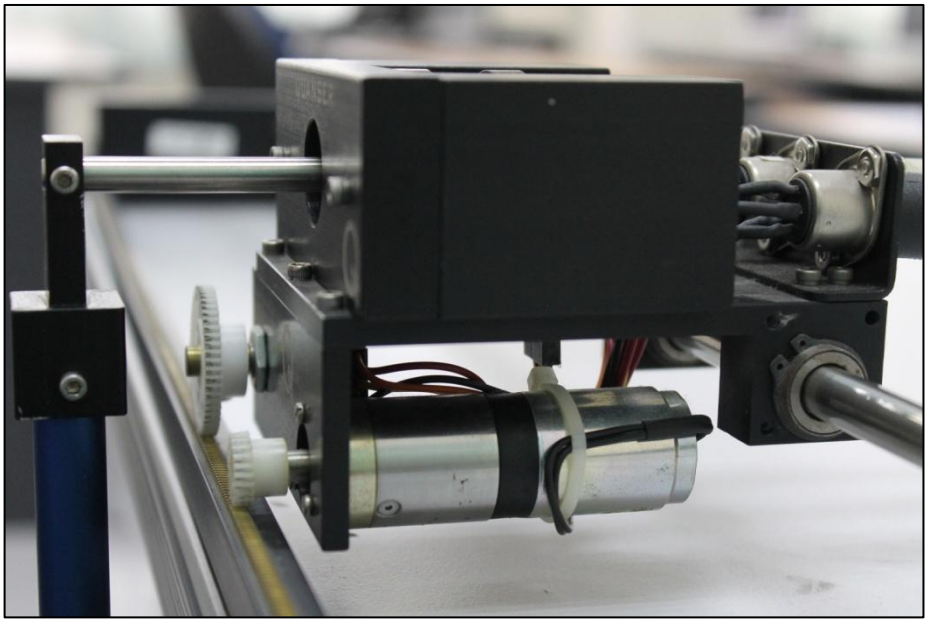

Figure 6.2: CIP cart with DC motor.

6.2.2 Real time controller setup

The controller setup contains Personal Computers (PC) and AD/DA data accusation card (model Q8, 14 bit with encoder inputs). The acquisition card is supplied with a terminal board where the encoders are connected directly, as it is shown in Figure 6.3. The Control algorithms are realized with Matlab Simulink, Fuzzy logic tool box and QuaRC real-time toolbox developed by Quanser, with clock frequency 1 kHz. The output control signal is amplified by Quanser power module (model UPM 800) in order to be applied directly on the DC motor, see Figure 6.4.

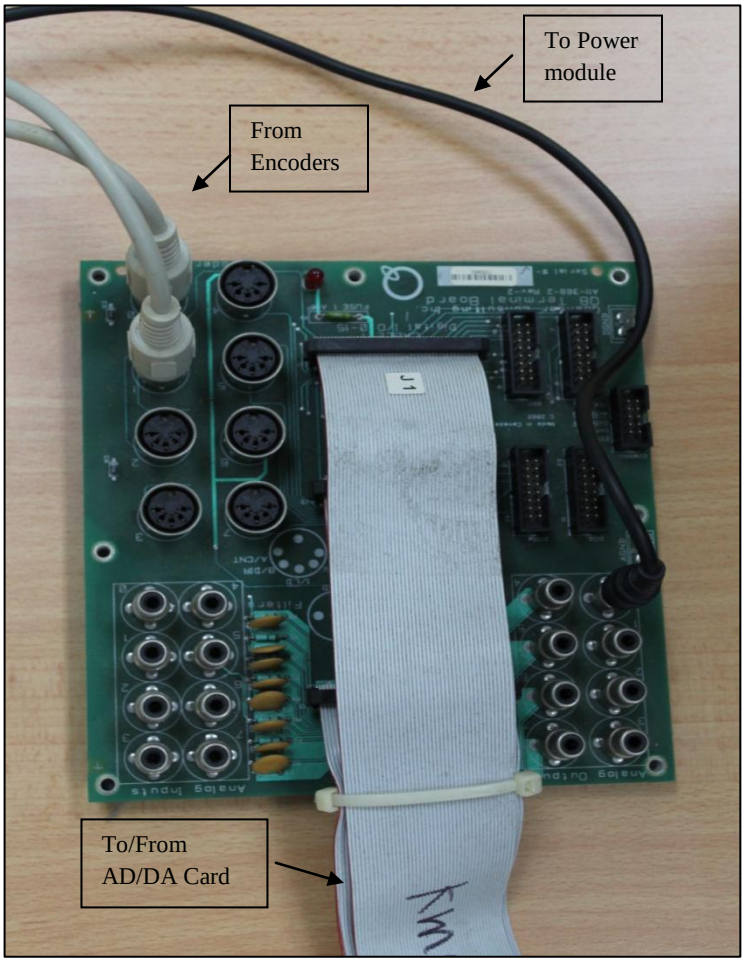

Figure 6.3: AD/DA card terminal board

Figure 6.4: Power module.

6.2.3 Velocity and acceleration estimation

The sensed values of the pendulum angular position and the cart position suffer from quantization errors due to encoder's measurements. The errors values will be enlarged in velocity and acceleration estimation, and affect the controller results (Han et al., 2007) . Thus, least square fitting algorithm is used to estimate velocities and acceleration for the cart and the pendulum. The velocity and acceleration values are estimated by a third order polynomial function. This function is established based on a least square fitting to the most

recent 8 measured values of the encoder counts. This fitting technique is also known as (LSF 3/8)(Brown et al., 1992). Schematic diagram for the fitting process is shown in Figure 6.5 , where ΔT is the sampling time and $T_{1\rightarrow 8}$ is the time for each sample.

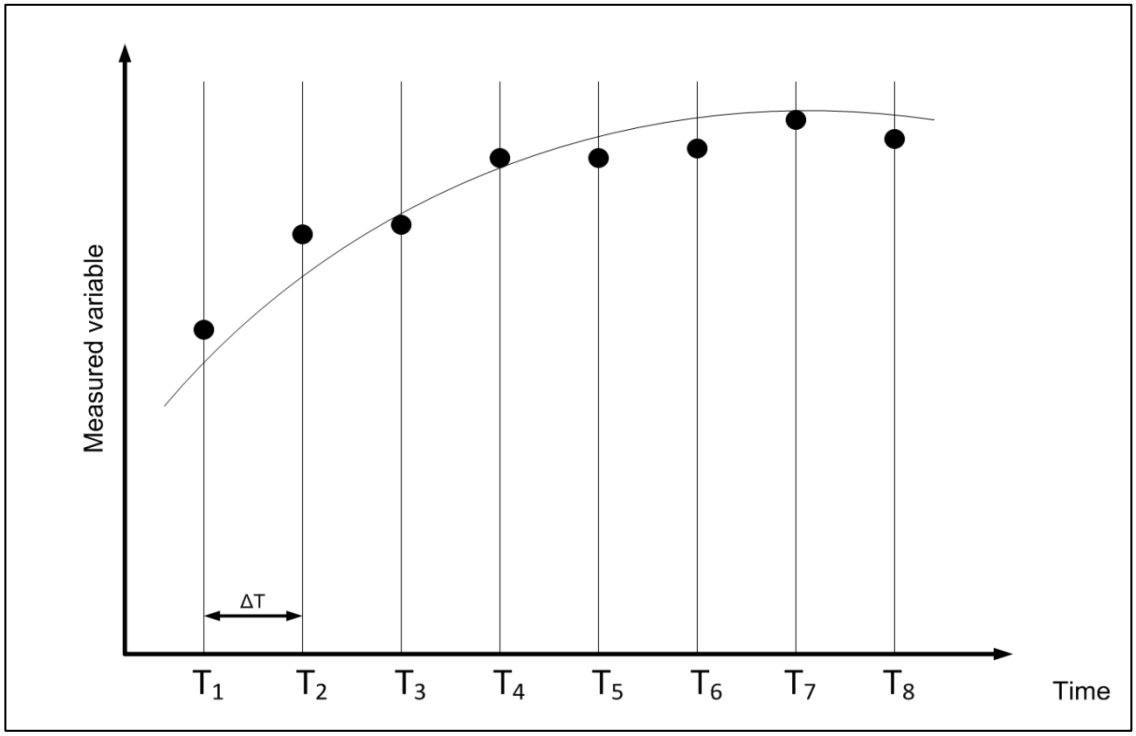

Figure 6.5: Schematic diagram for the fitting process.

6.3 Fuzzy swinging with SMC experimental results

For SMC real time implementation, the controller parameters are chosen to be C_1=4, C_2=2, K=5, $\Phi = 2.2x10^3$, Φ_z =4 and Z_u=0.9 . Figure 6.6-Figure 6.8 show the real implementation of fuzzy swing-up and with SMC. The pendulum is swung up within 6 seconds before the SMC is applied. The pendulum is balanced in the upward position where the stability could

be noticed. The cart displacement and control signal are driven near to the equilibrium point with small oscillation.

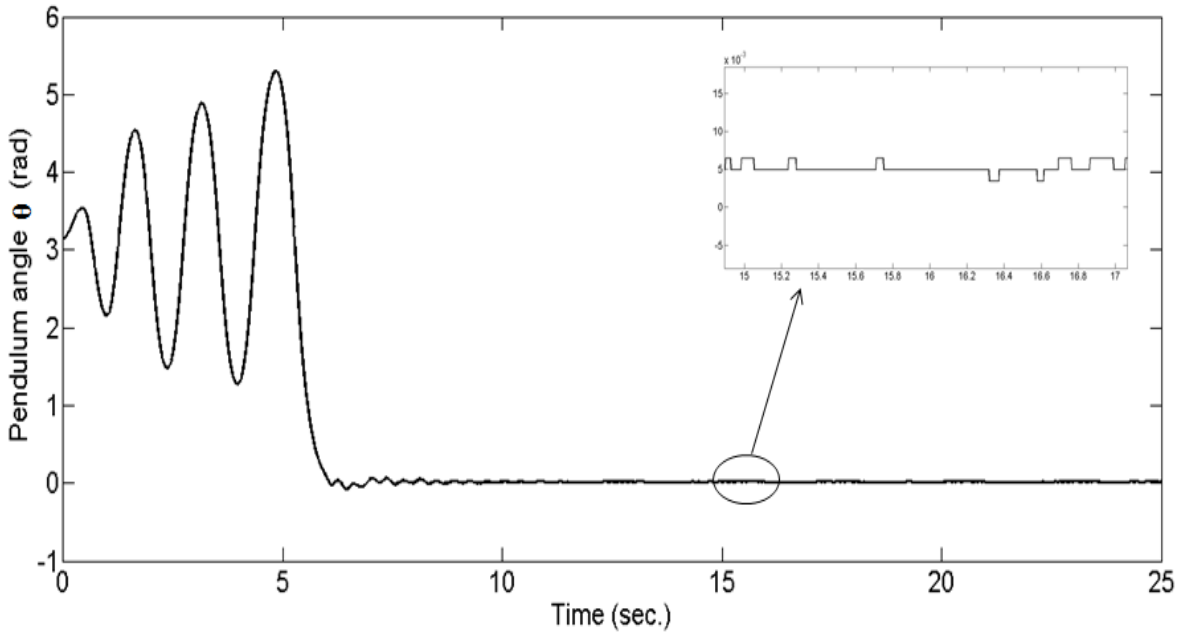

Figure 6.6: Experimental result for pendulum angular position with Fuzzy swing up and SMC.

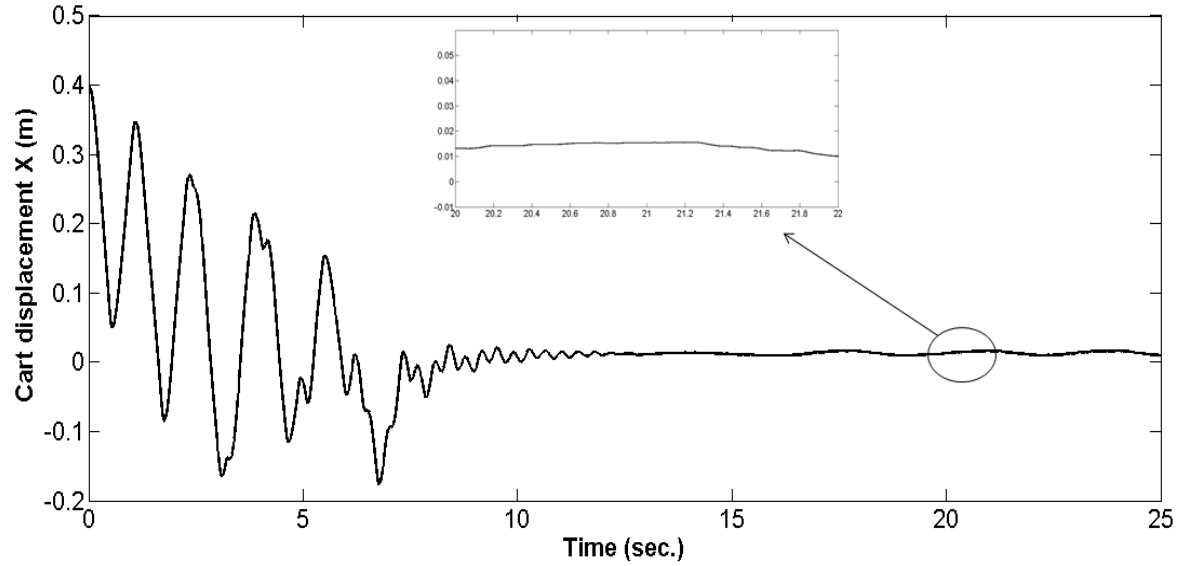

Figure 6.7:. Experimental result for cart position for Fuzzy swing up with SMC.

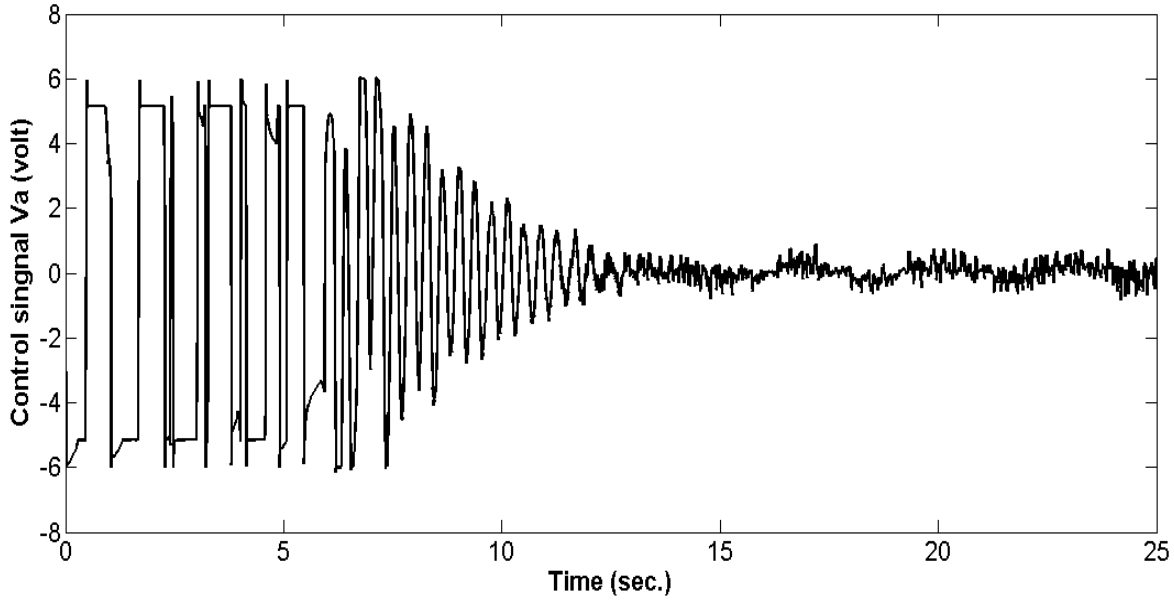

Figure 6.8: Experimental result for control voltage for Fuzzy swing up with SMC.

6.4 Fuzzy swinging with LQR experimental results

For LQRC, the selected controller parameters are, R=diag[400 1 2500 1], Q= 1 and the generated feedback gain vector K_L=[-20 -21.6 124.96 23.2]. In Figure 6.9, the fuzzy swing-up is tasted with LQRC, the results show that the pendulum takes 6 second to reach the upward position, before the stabilization LQRC is applied. For the steady state response, some oscillations could be noticed in the pendulum angle response because of the friction effects and other uncertainty sources. In Figure 6.10, the cart response shows oscillations and steady state error. Figure 6.11 shows the control signal for LQRC, where a high overshoot values could be seen.

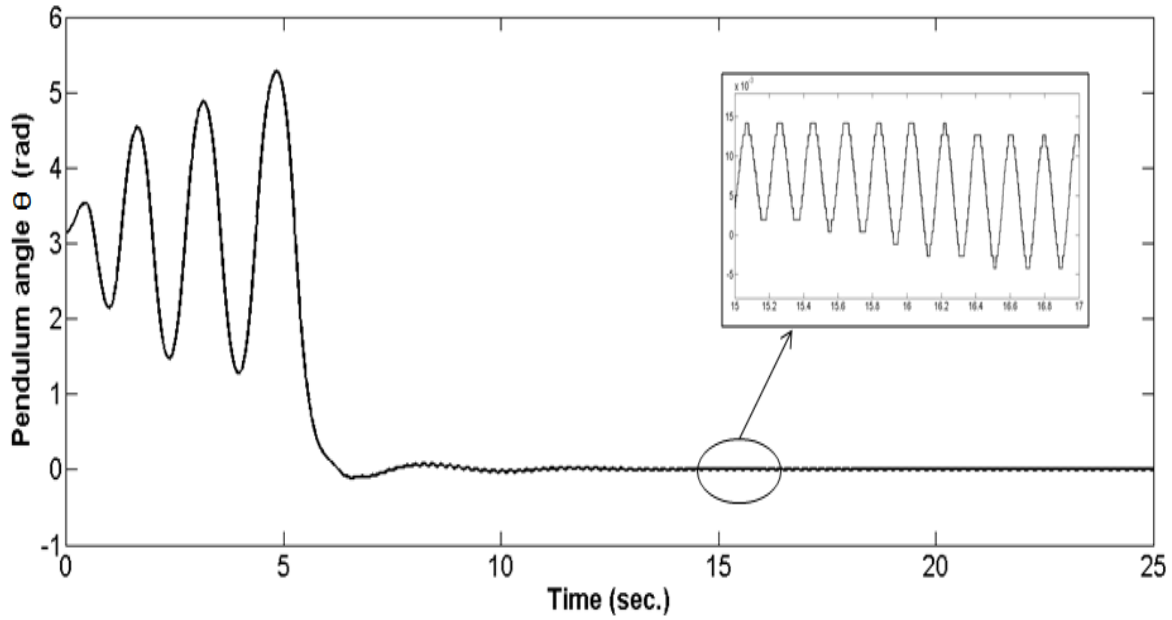

Figure 6.9: Experimental result for pendulum angular position with Fuzzy swing up with LQRC.

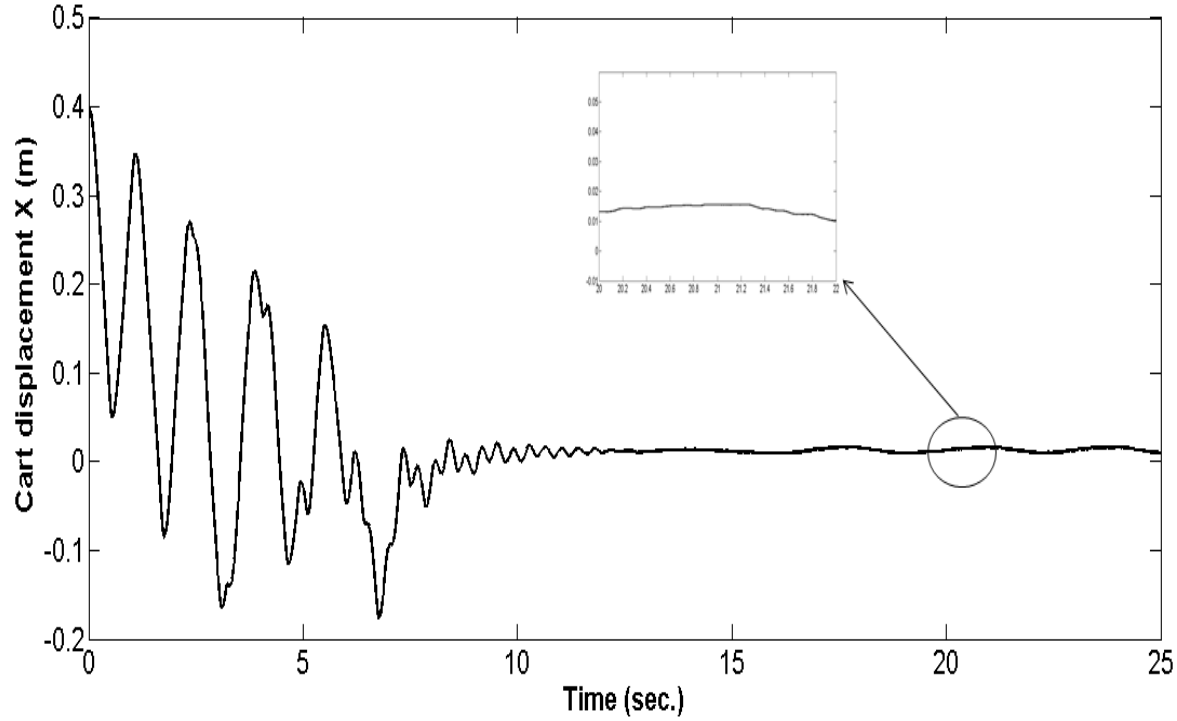

Figure 6.10: Experimental result for cart position with Fuzzy swing up with LQRC.

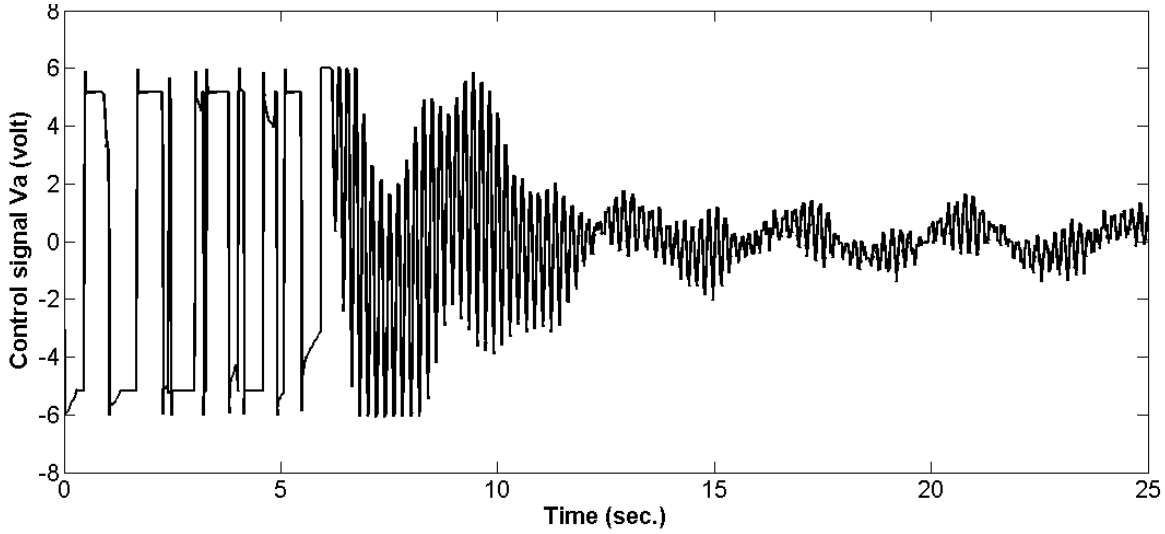

Figure 6.11: Experimental result for control voltage for Fuzzy swing up with LQRC.

Chapter Seven

7 Comparison results and discussion

7.1 Introduction

A comparison study has been performed between the proposed SMC and LQRC. The aim of this comparison is to show the SMC effectiveness in achieving the stability under external disturbances, and in the real implementation. This comparison also shows the robustness of the proposed controller comparing with other published techniques (Chatterjee, et al., 2002; Muskinja andTovornik, 2006).

7.2 Simulation comparison

In order to test the controller robustness, an external disturbance, with value of 0.1 rad and one second duration, has been applied after 20 seconds. The pendulum and cart responses are shown in Figure 7.1 and Figure 7.2, respectively. The pendulum angular response shows faster response for SMC and ability to reject the disturbance much more efficiently than LQRC. The maximum overshoot has been reduced by 30% when SMC is applied. The cart response shows the robustness of the SMC over LQRC where the maximum overshoot has been increased by 100% using LQR instead of SMC. Furthermore, in LQRC, the cart has exceeded the rail limits.

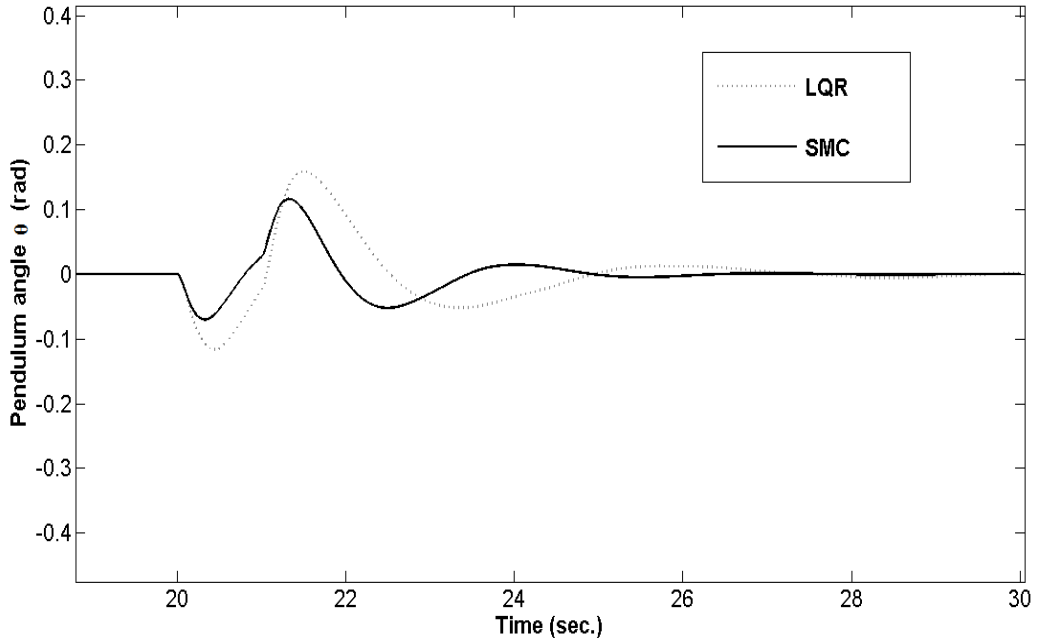

Figure 7.1 : Pendulum angular position response under disturbance.

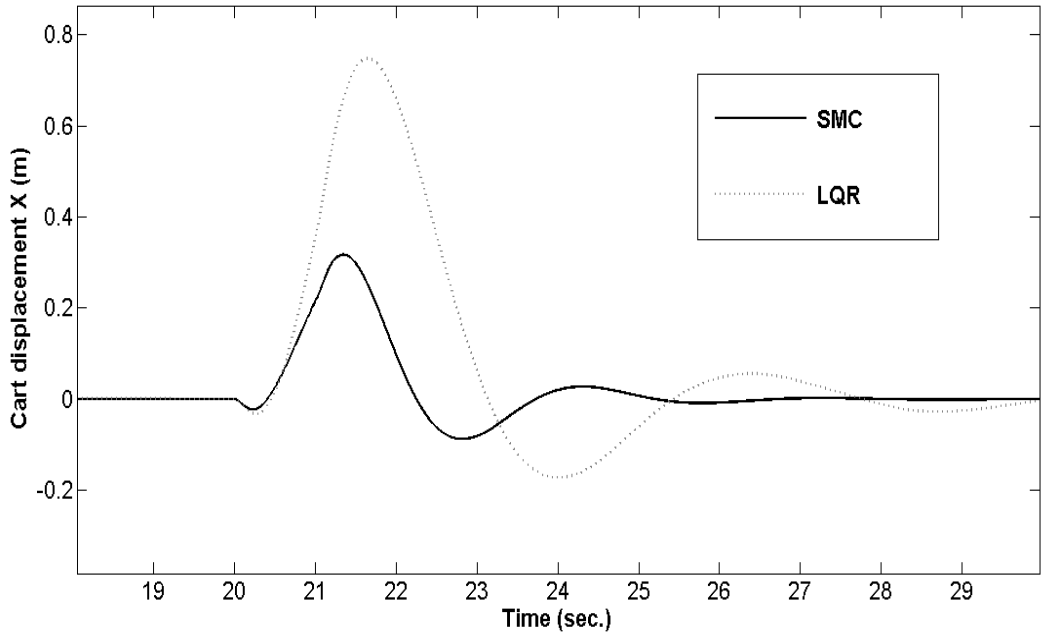

Figure 7.2: Cart position response under disturbance.

7.3 Experimental comparison

For the real implementation, SMC and LQRC steady state responses are compared. Figure 7.3 clearly shows that the pendulum angle steady state oscillations are significantly decreased by using SMC. The maximum overshoot is only 2 encoder counts whereas it reaches 10 counts for LQRC. Steady state error with value of 0.04 rad could be noticed due to sensor resolution. The cart displacement comparison is seen in Figure 7.4. The steady state error is increased three times with LQRC and higher frequencies could be observed comparing with SMC. Again, it is obviously seen in Figure 7.5 that SMC is capable of stabilizing the system with less control signal noise and lower consumed power as well.

Comparison results show the effectiveness of the proposed SMC however, more enhanced results could be achieved by using higher resolution sensors. For SMC, the controller robustness could be improved by using acceleration sensors since it is not considered in this controller implementation because of high noises.

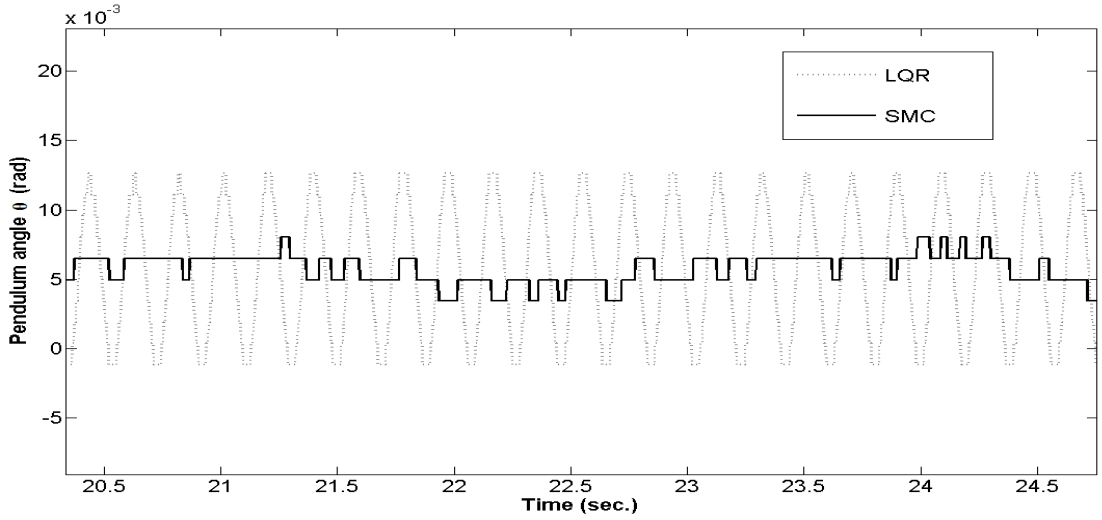

Figure 7.3: Pendulum angle experimental result.

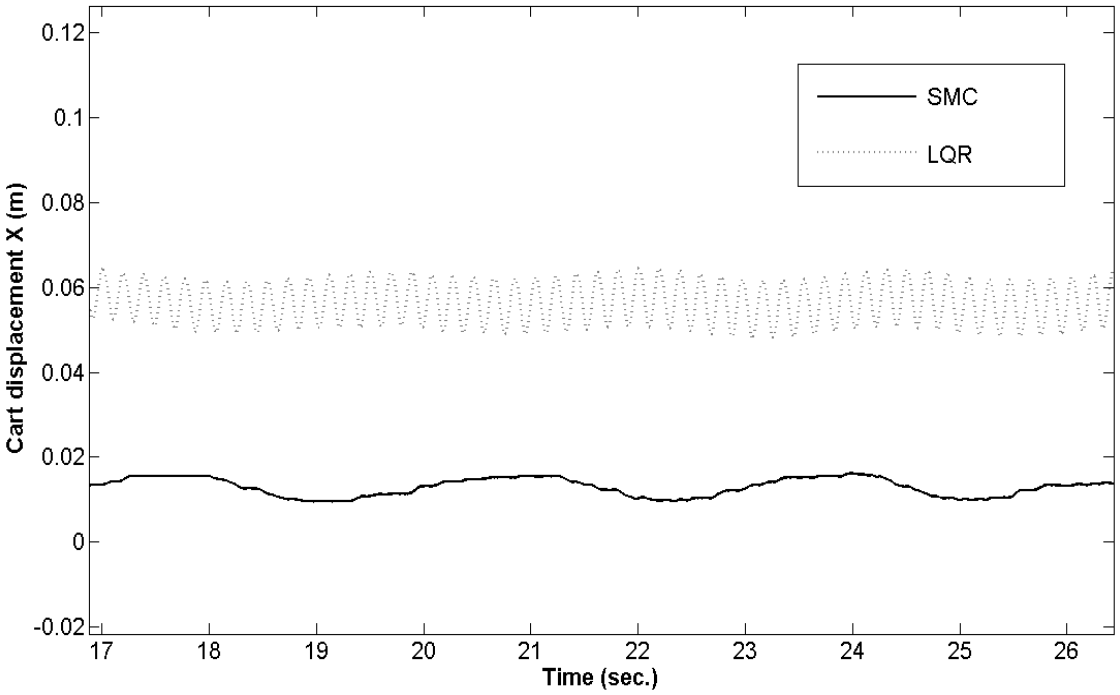

Figure 7.4: Cart position experimental result.

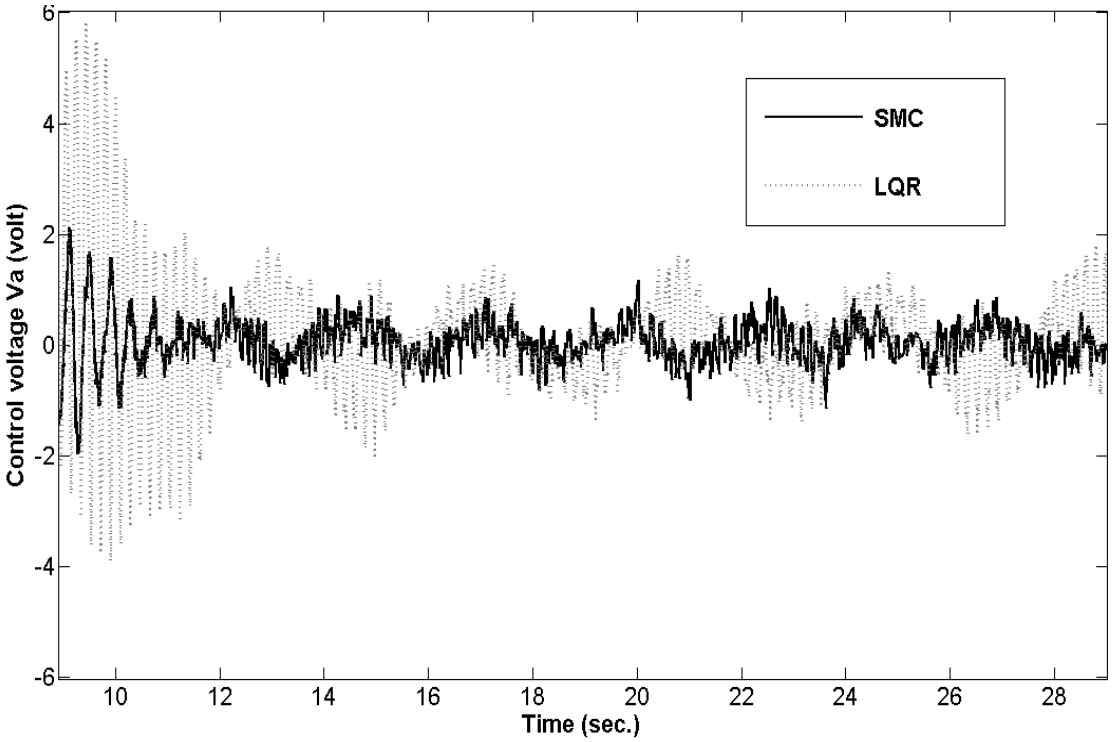

Figure 7.5:. Control voltage experimental result.

Chapter Eight

8 Conclusion and Future work

8.1 Conclusion

In this study, fuzzy swing-up with sliding mode controller has been developed for swinging up and stabilization the cart-inverted pendulum system. In the system model, two third order differential equations have been derived to combine the DC motor dynamics with CIP mechanics in one model. For testing purpose, nonlinear friction force between the cart and the rail has been added to the model equation. A fuzzy swing-up controller is designed to swing the pendulum within the cart rail limits. The proposed controller is designed based on 30 fuzzy (If-Then) rules, where the controller inputs are the pendulum angle, the pendulum angular velocity and the cart position. Whereas, the output is the DC-motor applied voltage. Once the pendulum reaches the upward position, the control algorithm gives a trigger signal to one-move switch to switch between the swinging-up and stabilization states. For system stabilization, SMC has been designed based on the derived model, where the overall system stability is guaranteed. For comparison purposes, LQRC has been designed to be compared with the proposed SMC.

Simulation results reviled that, the proposed SMC is effective and robust. The controllers have been applied on a real CIP system and tested experimentally. The experimental results have shown a significant improvement for SMC in terms of system stability, steady state

error and steady state oscillations. The cart position steady state error was decreased by 60% with low frequencies oscillation when applying SMC in place to LQRC.

8.2 Future work

Although the proposed SMC meets the study objectives, some points might be considered for future investigation.

The experimental results could be improved by using accelerometers for acceleration sensing in order to decrease the acceleration noise, since the accelerations have been estimated based on least square fitting for the encoder counts.

The proposed controller could be generalized and applied on any two degrees of freedom underactuated robots, two wheel mobile robot and any multi-degree of freedom under actuated system. In addition the controller the controller might be extended to be applied on a double inverted pendulum system.

Other control algorithm like neuro-fuzzy control might be applied and compared with the proposed SMC. For implementation, low cost DSP real time controller instead of the real time PC.

References

Armstrong-Hélouvry, B., Dupont, P., & De Wit, C. C. (1994). A survey of models, analysis tools and compensation methods for the control of machines with friction. *Automatica, 30*(7), 1083-1138.

Åström, K. J., & Furuta, K. *Swinging up a Pendulum by Energy Control.* 13th IFAC World Congress, San Francisco, USA

Åström, K. J., & Furuta, K. (2000). Swinging up a pendulum by energy control. *Automatica, 36*(2), 287-295.

Bartoszewicz, A., & Nowacka-Leverton, A. (2010). ITAE Optimal Sliding Modes for Third-Order Systems With Input Signal and State Constraints. *IEEE Trans. Autom. Control, 55*(8), 1928-1932.

Barya, K., Tiwari, S., & Jha, R. *Comparison of LQR and robust controllers for stabilizing inverted pendulum system.* EEE International Conference on Communication Control and Computing Technologies (ICCCCT), 2010 7-9 Oct. 2010

Boiko, I., & Fridman, L. (2005). Analysis of chattering in continuous sliding-mode controllers. *IEEE Transactions on Automatic Control, 50*(9), 1442-1446.

Brown, R. H., Schneider, S. C., & Mulligan, M. G. (1992). Analysis of algorithms for velocity estimation from discrete position versus time data. *IEEE Trans. Ind. Electron., 39* 11-19.

Buckingham, R. (2003). "Super mechano systems"–a report on the IEE Tustin/UKACC annual lecture given by Professor Katsuhisha Furuta. *Industrial Robot: An International Journal, 30*(5), 417-421.

Bugeja, M. *Non-linear swing-up and stabilizing control of an inverted pendulum system.* EUROCON 2003. Computer as a Tool. The IEEE Region 8, 22-24 Sept. 2003

Campbell, S. A., Crawford, S., & Morris, K. (2008). Friction and the inverted pendulum stabilization problem. *Journal of Dynamic Systems Measurement and Control-Transactions of the Asme, 130*(5).

Cardozo, G. S. S., & Vera, L. M. S. *Prototype for a Self-Balanced Personal Transporter*. Engineering Applications (WEA), 2012 Workshop on, 2-4 May 2012

Chatterjee, D., Patra, A., & Joglekar, H. K. (2002). Swing-up and stabilization of a cart–pendulum system under restricted cart track length. *Systems & Control Letters*, *47*(4), 355-364.

Das, S. K., & Paul, K. K. (2011). Robust compensation of a Cart–Inverted Pendulum system using a periodic controller: Experimental results. *Automatica*, *47*(11), 2543-2547.

Edwards, C., & Spurgeon, S. K. (1998). *Sliding mode control : theory and applications*. London: Taylor & Francis.

El-Hawwary, M. I., Elshafei, A. L., Emara, H. M., & Fattah, H. A. A. (2006). Adaptive fuzzy control of the inverted pendulum problem. *IEEE Transactions on Control Systems Technology*, *14*(6), 1135-1144.

Elsayed, B. A., Hassan, M. A., & Mekhilef, S. (2013). Decoupled Third-order Fuzzy Sliding Model Control For Cart-Inverted Pendulum System. *Appl. Math. Inf. Sci.*, *7*(1), 253-261.

Faizan, F., Farid, F., Rehan, M., Mughal, S., & Qadri, M. T. *Implementation of discrete PID on Inverted pendulum.* 2nd International Conference on Education Technology and Computer (ICETC), 2010 22-24 June 2010

Fallahi, M., & Azadi, S. *Adaptive Control of an Inverted Pendulum Using Adaptive PID Neural Network.* 2009 International Conference on Signal Processing Systems, 15-17 May 2009

Fujinaka, T., Kishida, Y., Yoshioka, M., & Omatu, S. *Stabilization of double inverted pendulum with self-tuning neuro-PID.* Proceedings of the IEEE-INNS-ENNS International Joint Conference on Neural Networks, 2000. IJCNN 2000, 2000

Furuta, K., Okutani, T., & Sone, H. (1978). Computer control of a double inverted pendulum. *Computers & Electrical Engineering*, *5*(1), 67-84.

Furuta, K., Yamakita, M., & Kobayashi, S. *Swing up control of inverted pendulum.* International Conference on Industrial Electronics, Control and Instrumentation, IECON '91, 28 Oct-1 Nov 1991

Furuta, K., Yamakita, M., & Kobayashi, S. (1992). Swing-up control of inverted pendulum using pseudo-state feedback. *Journal of Systems and Control Engineering, 206*, 263-269.

Han, J. D., He, Y. Q., & Xu, W. L. (2007). Angular acceleration estimation and feedback control: An experimental investigation. *Mechatronics, 17*(9), 524-532.

Hung, L. C., & Chung, H. Y. (2007). Decoupled control using neural network-based sliding-mode controller for nonlinear systems. *Expert Systems with Applications, 32*(4), 1168-1182.

Itkis, U. (1976). *Control systems of variable structure*. New York: Wiley.

Ji-Chang, L., & Ya-Hui, K. (1998). Decoupled fuzzy sliding-mode control. *Fuzzy Systems, IEEE Transactions on, 6*(3), 426-435.

Khalil, H. K. (2002). *Nonlinear systems* (3rd ed.). Upper Saddle River, N.J.: Prentice Hall.

La Hera, P. X., Freidovich, L. B., Shiriaev, A. S., & Mettin, U. (2009). New approach for swinging up the Furuta pendulum: Theory and experiments. *Mechatronics, 19*(8), 1240-1250.

Liang, Y., & Jianying, Y. *Robust continuous sliding mode control for aerodynamic missile using stable system center technique.* 3rd International Symposium on Systems and Control in Aeronautics and Astronautics (ISSCAA), 2010 8-10 June 2010

Lin, C. M., & Mon, Y. J. (2005). Decoupling control by hierarchical fuzzy sliding-mode controller. *IEEE Transactions on Control Systems Technology, 13*(4), 593-598.

Lo, J. C., & Kuo, Y. H. (1998). Decoupled fuzzy sliding-mode control. *IEEE Transactions on Fuzzy Systems, 6*(3), 426-435.

Mason, P., Broucke, M., & Piccoli, B. (2008). Time optimal swing-up of the planar pendulum. *IEEE Transactions on Automatic Control, 53*(8), 1876-1886.

Mason, P., Broucke, M. E., & Piccoli, B. *Time optimal swing-up of the planar pendulum.* Proceedings of the 46th IEEE Conference on Decision and Control, Vols 1-14

Mondal, S., Gokul, T. V., & Mahanta, C. *Chattering free sliding mode controller for mismatched uncertain system.* 7th IEEE International Conference on Industrial and Information Systems (ICIIS), 2012 6-9 Aug. 2012

Mori, S., Nishihara, H., & Furuta, K. (1976). Control of unstable mechanical system Control of pendulum†. *International Journal of Control, 23*(5), 673-692.

Muskinja, N., & Tovornik, B. (2006). Swinging up and stabilization of a real inverted pendulum. *IEEE Transactions on Industrial Electronics, 53*(2), 631-639.

Ogata, K. (2002). *Modern control engineering* (4th ed.). Upper Saddle River, NJ: Prentice Hall.

Olsson, H., Astrom, K. J., de Wit, C. C., Gafvert, M., & Lischinsky, P. (1998). Friction models and friction compensation. *Eur. J. Control, 4*(3), 176-195.

Palm, R., Driankov, D., & Hellendoorn, H. (1997). *Model based fuzzy control : fuzzy gain schedulers and sliding mode fuzzy controllers*. Berlin ; New York: Springer.

Park, D., Chwa, D., & Hong, S. K. *An estimation and compensation of the friction in an inverted pendulum.* 2006 SICE-ICASE International Joint Conference, Vols 1-13

Park, M. S., & Chwa, D. (2009). Swing-Up and Stabilization Control of Inverted-Pendulum Systems via Coupled Sliding-Mode Control Method. *IEEE Transactions on Industrial Electronics, 56*(9), 3541-3555.

Passino, K. M., & Yurkovich, S. (1998). *Fuzzy control*. Menlo Park, Calif.: Addison-Wesley.

Prasad, L. B., Tyagi, B., & Gupta, H. O. *Optimal control of nonlinear inverted pendulum dynamical system with disturbance input using PID controller & LQR.* IEEE International Conference on Control System, Computing and Engineering (ICCSCE), 2011, 25-27 Nov. 2011

Prasad, L. B., Tyagi, B., & Gupta, H. O. *Modelling and Simulation for Optimal Control of Nonlinear Inverted Pendulum Dynamical System Using PID Controller and LQR.* Sixth Asia Modelling Symposium (AMS), 2012 29-31 May 2012

Rani, M. R., Selamat, H., Zamzuri, H., & Ahmad, F. *PID controller optimization for a rotational inverted pendulum using genetic algorithm.* 4th International Conference on Modeling, Simulation and Applied Optimization (ICMSAO), 2011, 19-21 April 2011

Rubi, J., Rubio, A., & Avello, A. (2002). Swing-up control problem for a self-erecting double inverted pendulum. *IEE Proceedings -Control Theory and Applications, 149*(2), 169-175.

Segway. (2012). Segway Robot. from http://www.segway.com/business/products-solutions/index.php

Shiriaev, A. S., Egeland, O., Ludvigsen, H., & Fradkov, A. L. (2001). VSS-version of energy-based control for swinging up a pendulum. *Systems & Control Letters, 44*(1), 45-56.

Shiriaev, A. S., Freidovich, L. B., Robertsson, A., Johansson, R., & Sandberg, A. (2007). Virtual-Holonomic-Constraints-Based Design of Stable Oscillations of Furuta Pendulum: Theory and Experiments. *IEEE Transactions on Robotics, 23*(4), 827-832.

Siew-Chong, T., Lai, Y. M., & Tse, C. K. (2008). Indirect Sliding Mode Control of Power Converters Via Double Integral Sliding Surface. *IEEE Transactions on Power Electronics, 23*(2), 600-611.

Sugie, T., & Fujimoto, K. *Control of inverted pendulum systems based on approximate linearization: design and experiment.* Proceedings of the 33rd IEEE Conference on Decision and Control, 1994, 14-16 Dec 1994

Tao, C. W., Taur, J. S., Hsieh, T. W., & Tsai, C. L. (2008). Design of a Fuzzy Controller With Fuzzy Swing-Up and Parallel Distributed Pole

Assignment Schemes for an Inverted Pendulum and Cart System. *IEEE Transactions on Control Systems Technology, 16*(6), 1277-1288.

Tao, C. W., Taur, J. S., Wang, C. M., & Chen, U. S. (2008). Fuzzy hierarchical swing-up and sliding position controller for the inverted pendulum-cart system. *Fuzzy Sets and Systems, 159*(20), 2763-2784.

Tedrake, R. (2009). Underactuated Robotics. *(Massachusetts Institute of Technology: MIT OpenCourseWare)*, from http://ocw.mit.edu

Utkin, V. (1977). Variable structure systems with sliding modes. *IEEE Transactions on Automatic Control, 22*(2), 212-222.

Voth, D. (2005). Segway to the future [autonomous mobile robot]. *IEEE Expert / IEEE Intelligent Systems - EXPERT 20*(3), 5-8.

Wang, W., Liu, X. D., & Yi, J. Q. (2007). Structure design of two types of sliding-mode controllers for a class of under-actuated mechanical systems. *Control Theory & Applications, IET, 1*(1), 163-172.

Wei, Q., Dayawansa, W. P., & Levine, W. S. (1995). Nonlinear controller for an inverted pendulum having restricted travel. *Automatica, 31*(6), 841-850.

Wongsathan, C., & Sirima, C. *Application of GA to design LQR controller for an Inverted Pendulum System.* IEEE International Conference on Robotics and Biomimetics, 2008. ROBIO 2008. , 22-25 Feb. 2009

Xiuli, Y., Shimin, W., & Lei, G. *Cascade Sliding Mode Control for Bicycle Robot.* International Conference on Artificial Intelligence and Computational Intelligence (AICI), 2010 23-24 Oct. 2010

Yang, J. H., Shim, S. Y., Seo, J. H., & Lee, Y. S. (2009). Swing-up Control for an Inverted Pendulum with Restricted Cart Rail Length. *International Journal of Control Automation and Systems, 7*(4), 674-680.

Yorgancioglu, F., & Komurcugil, H. (2010). Decoupled sliding-mode controller based on time-varying sliding surfaces for fourth-order systems. *Expert Systems with Applications, 37*(10), 6764-6774.

Young, K. D., & Drakunov, S. V. *Sliding Mode Control with Chattering Reduction.* American Control Conference, 1992, 24-26 June 1992

Zadeh, L. A. (1965). Fuzzy sets. *Information and Control*, *8*(3), 338-353.

Zadeh, L. A. (1973). Outline of a New Approach to the Analysis of Complex Systems and Decision Processes. *IEEE Transactions on Systems, Man and Cybernetics., SMC-3*(1), 28-44.

Appendix 1

DC Motor specification sheet

Series 2338 ... S

		2338 S	4.5 S	006 S	009 S	012 S	018 S	024 S	
1	Nominal voltage	U_N	4.5	6	9	12	18	24	Volt
2	Terminal resistance	R ± 12%	1.4	2.6	5.7	10.0	23.5	38.0	Ω
3	Output power	$P_{2\,max.}$	3.39	3.23	3.29	3.31	3.18	3.50	W
4	Efficiency	$\eta_{max.}$	70	69	67	66	67	67	%
5	No-load speed	n_0 ± 12%	7,200	7,200	7,400	7,800	7,400	7,600	rpm
6	No-load current (with shaft ø 0.12 in)	I_0 ± 50%	0.100	0.080	0.060	0.050	0.030	0.025	A
7	Stall torque	M_H	2.55	2.42	2.41	2.29	2.32	2.49	oz-in
8	Friction torque	M_R	0.082	0.086	0.095	0.099	0.095	0.102	oz-in
9	Speed constant	k_n	1,650	1,240	855	678	428	330	rpm/V
10	Back-EMF constant	k_E	0.606	0.804	1.170	1.470	2.340	3.030	mV/rpm
11	Torque constant	k_M	0.818	1.088	1.586	1.997	3.158	4.107	oz-in/A
12	Current constant	k_I	1.222	0.919	0.630	0.501	0.317	0.244	A/oz-in
13	Slope of n-M curve	Δn/ΔM	2,824	2,975	3,071	3,406	3,190	3,052	rpm/oz-in
14	Rotor inductance	L	100	180	380	630	1,400	2,600	µH
15	Mechanical time constant	τ_m	20	17	17	17	17	17	ms
16	Rotor inertia	J	$6.797 \cdot 10^{-5}$	$5.523 \cdot 10^{-5}$	$5.240 \cdot 10^{-5}$	$4.815 \cdot 10^{-5}$	$5.098 \cdot 10^{-5}$	$5.381 \cdot 10^{-5}$	oz-in-sec²
17	Angular acceleration	$\alpha_{max.}$	38	44	46	48	46	47	$\cdot 10^3$rad/s²
18	Thermal resistance	$R_{th\,1}$ / $R_{th\,2}$	3 / 24						°C/W
19	Thermal time constant	τ_{w1} / τ_{w2}	5.7 / 645						s
20	Operating temperature range:								
	– motor		– 30 to +85 (– 22 to +185)						°C (°F)
	– rotor, max. permissible		+125 (+257)						°C (°F)
	Note: Special operating temperature models for		–55°C to +125°C (– 67°F to +257°F) available on request.						
21	Shaft bearings		sintered bronze sleeves		ball bearings		ball bearings, preloaded		
22	Shaft load max.:		(standard)		(optional)		(optional)		
	– with shaft diameter		0.1181		0.1181		0.1181		in
	– radial at 3,000 rpm (0.12 in from bearing)		9		72		72		oz
	– axial at 3,000 rpm		1.08		7.2		7.2		oz
	– axial at standstill		72		72		72		oz
23	Shaft play:								
	– radial	≤	0.0012		0.0006		0.0006		in
	– axial	≤	0.0079		0.0079		0		in
24	Housing material		steel, zinc galvanized and passivated						
25	Weight		2.47						oz
26	Direction of rotation		clockwise, viewed from the front face						
Recommended values									
27	Speed up to	$n_{e\,max.}$	6,000	6,000	6,000	6,000	6,000	6,000	rpm
28	Torque up to	$M_{e\,max.}$	0.566	0.566	0.566	0.566	0.566	0.566	oz-in
29	Current up to (thermal limits)	$I_{e\,max.}$	1.380	1.000	0.680	0.510	0.330	0.260	A

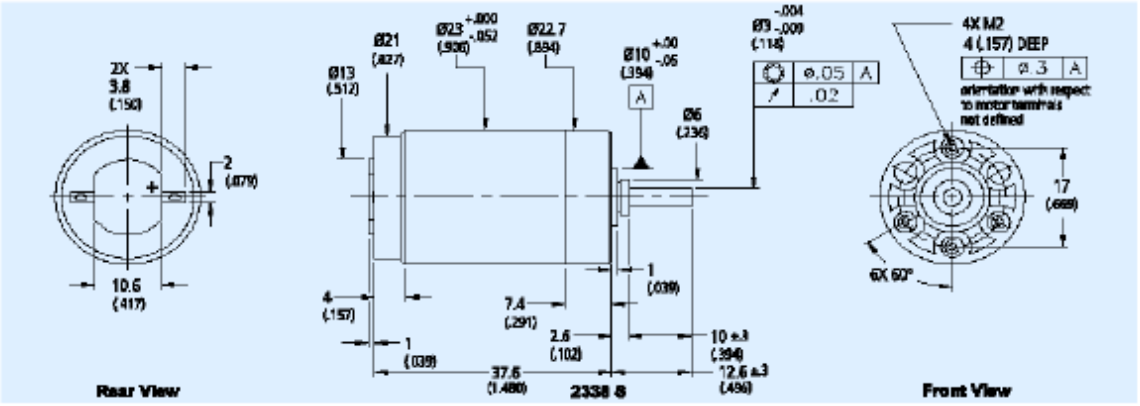

Encoder specification sheet

S1 & S2 Optical Shaft Encoders

Description:

The **S1** and **S2** series optical shaft encoders are non-contacting rotary to digital converters. Useful for position feedback or manual interface, the encoders convert real-time shaft angle, speed, and direction into TTL-compatible quadrature outputs with or without index. The encoders utilize an unbreakable mylar disk, metal shaft and bushing, LED light source, and monolithic electronics. They may operate from a single +5VDC supply.

The **S1** and **S2** encoders are available with ball bearings for motion control applications or torque-loaded to feel like a potentiometer for front-panel manual interface.

Electrical Specifications:
B leads A for clockwise shaft rotation, A leads B for counter clockwise shaft rotation viewed from the shaft/bushing side of the encoder. For complete details see our **HEDS** data sheet.

Features:

- Small size
- Low cost
- 2-channel quadrature, TTL square wave outputs
- 3rd channel index option
- Tracks from 0 to 100,000 cycles/sec
- Ball bearing option tracks to 10,000 RPM
- -40 to +100°C operating temperature
- Single +5V supply
- US Digital warrants its products against defects and workmanship for two years. See complete warranty for details.

Mechanical Specifications:

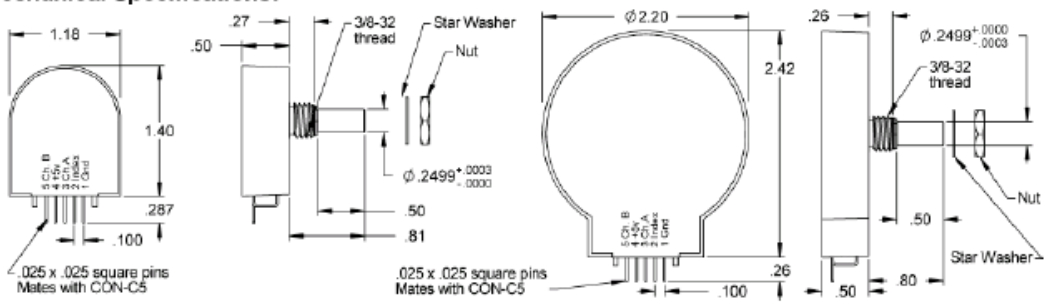

Mechanical Notes: (ball bearing)

Acceleration	10,000 rad/sec²
Vibration	20 g. 5 to 2KHz
Shaft Speed	10,000 RPM max. continuous
Acceleration	50K rad/sec² 10K rad/sec² (**S2** series)
Shaft Torque	0.05 in. oz. max.
Shaft Loading	1 lb. max.
Bearing Life	(40/P)³ = Life in millions of revs. P = radial load in pounds.
Weight	0.7 oz.
Shaft Runout	0.0015 T.I.R. max.

Mechanical Notes: (sleeve bushing)

Acceleration	10,000 rad/sec²
Vibration	20 g. 5 to 2KHz
Shaft Speed	100 RPM max. continuous
Shaft Rotation	Continuous & reversible
Shaft Torque	0.5 ±0.2 in. oz. 0.3 in. oz. max. (NT-option)
Shaft Loading	2 lbs. max. dynamic 20 lbs. max. static
Weight	0.7 oz.
Shaft Runout	0.0015 T.I.R. max.

Materials & Mounting:

Shaft	Brass or stainless
Bushing	Brass
Connector	Gold plated
Hole Diameter	0.375 in. +0.005 - 0
Panel Thickness	0.125 in. max.
Panel Nut Max Torque	20 in.-lbs.

Appendix 2

Matlab code for LQR controller

```
M=0.883;
m=0.2326;
L=0.3302;
I=7.88e-3;
Ra=2.6;
La=.18e-3;
J=3.9e-7;
B1=0;
r=6.35e-3;
b=0;
q1=0;
Km=0.00767;
Ke=.00767;
g=9.81;
%We have this two equation to find the state feedbak gains
% the first one is
%Va= A*xddot + B*xdot - c*theta + D*theta dot
% xddot = (-B/A)*xdot  + (C/A) theta - (D/A) thetadot  + (1/A) Va
A=(r*(M+m)*(Ra/Km))   +   ((J*Ra)/(r*Km)) -  ((r*m*m*L*L*Ra)/(Km*(I+(m*L*L))))
B=((r*b+(B1/r))*(Ra/Km))  +  (Ke/r)
C= (r*m*m*L*L*Ra*g)/(Km*(I+(m*L^2)))
D= (r*m*L*Ra*q1)/(Km*(I+(m*L^2)))
%the first equation will be
% the second equation is
%Va= F*thetaddot  -  G*theta + H*thetadot  + V* xdot
F= -((r*m*L*Ra)/Km) + (((r*(M+m)*(Ra/Km))+((J*Ra)/(r*Km)))*((I+m*L^2)/(m*L)))
G= ((r*(M+m)*(Ra/Km))+((J*Ra)/(r*Km))) * g
H= ((r*(M+m)*(Ra/Km))+((J*Ra)/(r*Km))) * (q1/(m*L))
V= ((r*b+(B1/r))*(Ra/Km))  +  (Ke/r)
%thesecond equation will be in form
% Thetaddot= (-V/F) xdot + (G/F) theta - (H/F) thetadot + (1/F) Va
AA=[0 1 0 0;0 (-B/A) (C/A) (-D/A) ;0 0 0 1;0 (-V/F) (G/F) (-H/F)]
BB=[0;(1/A)  ; 0 ; (1/F) ]
q=[ 1/((0.05)^2) 0 0 0  ; 0 1 0 0  ;0 0 1/((0.02)^2) 0 ;0 0 0 1 ]
r=[1/((0.5)^2)]
k = lqr(AA,BB,q,r)
```

Appendix 3

Simulink block for Fuzzy swing up with SMC controller

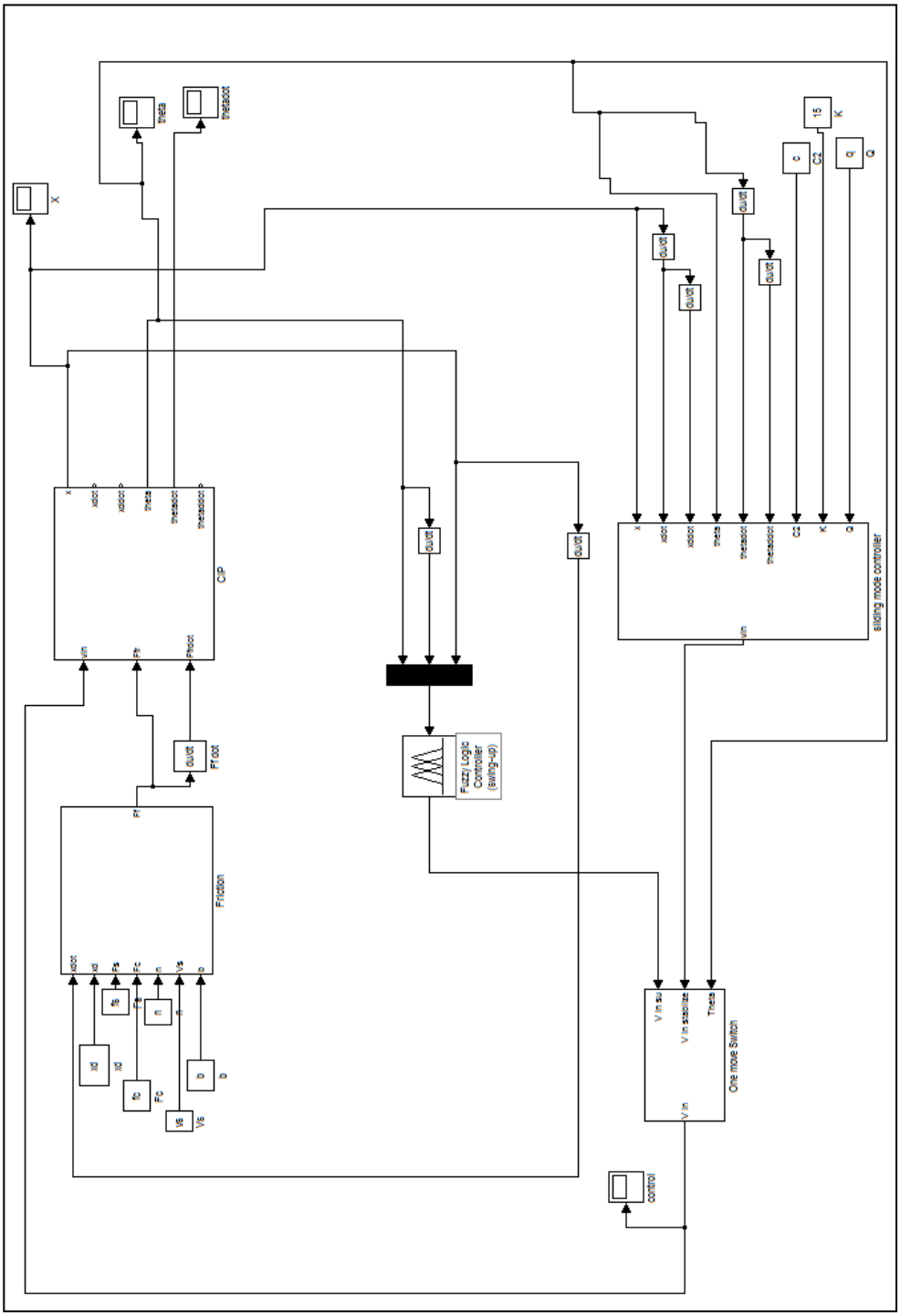

Simulink block for Fuzzy swing up with LQR controller

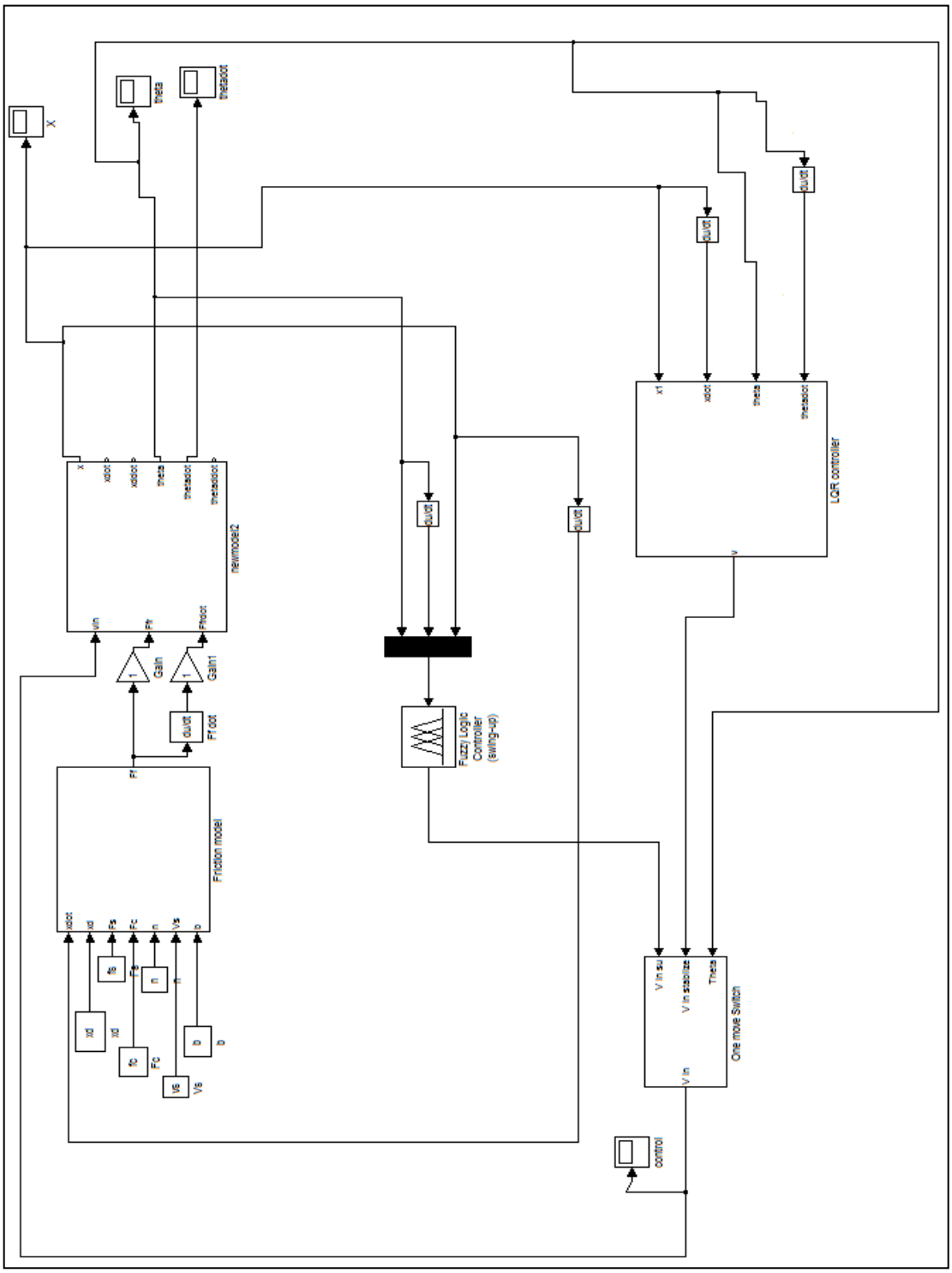

Appendix 4

Publication

- Belal A. Elsayed, M. A. Hassan and Saad Mekhilef, Decoupled Third-order Fuzzy Sliding Model Control For Cart-Inverted Pendulum System, Appl. Math. Inf. Sci. 7, No. 1, 193-201 (2013) (ISI cited publication)

- Belal A. Elsayed, M. A. Hassan and Saad Mekhilef, Fuzzy Swinging-up with Sliding Mode Control for Third Order Cart-Inverted Pendulum System, IEEE Transaction on Industrial Electronics.(2013) (Submitted)